Pre-aged plant waxes in tropical lake sediments and their influence on the chronology of molecular paleoclimate proxy records

Peter M. J. Douglas[1#*], Mark Pagani[1], Tim E. Eglinton[2,3], Mark Brenner[4], David A. Hodell[5], Jason H. Curtis[4], Keith Ma[1], and Andy Breckenridge[6]

[1]Department of Geology and Geophysics, Yale University, New Haven, CT, USA

[2]Department of Marine Chemistry and Geochemistry, Woods Hole Oceanographic Institution, Woods Hole, MA, USA

[3]Geological Institute, ETH Zurich, Zurich, Switzerland

[4]Department of Geological Sciences, University of Florida, Gainesville, FL, USA

[5]Godwin Laboratory for Palaeoclimate Research, Department of Earth Sciences, Cambridge University, Cambridge, UK

[6]Department of Natural Sciences, University of Wisconsin-Superior, Superior, WI, USA

Now at: Division of Geological and Planetary Sciences, California Institute of Technology, Pasadena, CA USA

*corresponding author: pdouglas@caltech.edu

Abstract: Sedimentary records of plant-wax hydrogen (δD_{wax}) and carbon ($\delta^{13}C_{wax}$) stable isotopes are increasingly applied to infer past climate change. Compound-specific radiocarbon analyses, however, indicate that long time lags can occur between the synthesis of plant waxes and their subsequent deposition in marginal marine sediments. The influence of these time lags on interpretations of plant-wax stable isotope records is presently unconstrained, and it is unclear whether such time lags also affect lacustrine sediments. We present compound-specific radiocarbon ($^{14}C_{wax}$) data for *n*-alkanoic acid plant waxes (*n*-C_{26} to *n*-C_{30}) from: 1) a sediment core from Lake Chichancanab, Yucatan Peninsula, Mexico, 2) soils in the Lake Chichancanab catchment, and 3) surface sediments from three other lakes in southeastern Mexico and northern Guatemala. $^{14}C_{wax}$ ages in the surface sediments are consistently older than modern, and may be negatively correlated with mean annual precipitation and positively correlated with lake catchment area. $^{14}C_{wax}$ ages in soils surrounding Lake Chichancanab increase with soil depth, consistent with deep, subsoil horizons being the primary source of lacustrine aged plant waxes, which are likely delivered to lake sediments through subsurface transport.

Plant waxes in the Lake Chichancanab core are 350 to 1200 years older than corresponding ages of bulk sediment deposition, determined by ^{14}C dates on terrestrial plant macrofossils in the core. A δD_{wax} time series is in closer agreement with other regional proxy hydroclimate records when a plant-wax ^{14}C age model is applied, as opposed to the macrofossil-based core chronology. Inverse modeling of plant-wax age distribution parameters suggests that plant waxes in the Lake Chichancanab sediment

core derive predominantly from millennial-age soil carbon pools that exhibit relatively little age variance (< 200 years).

Our findings demonstrate that high-temporal-resolution climate records inferred from stable isotope measures on plant waxes in lacustrine sediments may suffer from possible chronologic distortions as a consequence of long residence times of plant waxes in soils. They also underscore the importance of direct radiocarbon dating of these organic molecules.

1.Introduction

Carbon and hydrogen isotope compositions ($\delta^{13}C$ and δD) of plant waxes (long-carbon-chain *n*-alkyl lipids) are increasingly applied as tracers of past terrestrial climate change (Hughen et al., 2004; Pagani et al., 2006; Tipple and Pagani, 2010; Schefuss et al., 2011), with substantial attention on tropical lake sediments (Tierney et al., 2008; Tierney et al., 2010; Konecky et al., 2011; Tierney et al., 2011; Berke et al., 2012; Lane et al., 2014). Compound-specific isotope proxies have the potential to provide insights into past ecology, hydrology, and atmospheric water vapor dynamics across a range of timescales. Transport pathways of plant waxes from leaf surfaces to sedimentary basins, however, remain poorly understood.

A number of studies have measured the radiocarbon composition of plant waxes ($^{14}C_{wax}$) in sedimentary environments, with the intent to understand the age of terrigenous organic matter buried in marginal marine sediments (Smittenberg et al., 2004; Smittenberg et al., 2006; Drenzek et al., 2007; Mollenhauer and Eglinton, 2007; Drenzek et al., 2009; Kusch et al., 2010; Vonk et al., 2010; Galy and Eglinton, 2011; Feng et al.,

2012). These studies have typically found plant waxes in surface deposits to be hundreds to thousands of years older than the associated sediments, reflecting the input of pre-aged plant waxes, which derive largely from soil-carbon reservoirs (Smittenberg et al., 2006; Kusch et al., 2010; Vonk et al., 2010) and are transported by groundwater and surface runoff (Vonk et al., 2010; Feng et al., 2013). The only published study of $^{14}C_{wax}$ from lake sediments found relatively close agreement between plant-wax radiocarbon ages and the ages of terrigenous plant macrofossils, which are generally considered to reflect the timing of sediment deposition (Uchikawa et al., 2008). That study, however, did not include $^{14}C_{wax}$ data from the top of the sediment core, and not all $^{14}C_{wax}$ ages agreed with terrigenous macrofossil ^{14}C ages from nearby stratigraphic horizons. It seems likely that substantial contributions of pre-aged plant waxes to lake sediments are common in many environments and could complicate biomarker chronologies by introducing potentially significant time lags between lipid biosynthesis and lipid deposition in sediments (Drenzek et al., 2007; Galy et al., 2011; Li et al., 2011). In addition, mixing plant waxes of distinct ages within a given sediment horizon could lead to time-averaging or other distortions of plant-wax isotope records. To date, however, no studies have compared plant-wax radiocarbon ages with plant-wax stable isotope data from the same sediment sequence to assess such temporal distortions.

In this study, we present $^{14}C_{wax}$ and δD_{wax} data from a well-studied sediment core from Lake Chichancanab, Mexico (Figure 1A). We compare these data with an independent macrofossil-based ^{14}C sediment chronology and records of hydroclimate change from Lake Chichancanab and other nearby localities, to examine potential contributions of pre-aged plant waxes and establish if they introduce temporal distortions

in δD_{wax}-hydroclimate records. We performed inverse modeling analyses to determine what plant-wax age distributions are most consistent with Lake Chichancanab $^{14}C_{wax}$ and δD_{wax} data. We also analyzed $\Delta^{14}C_{wax}$ values in surficial sediments from three other lakes to assess variability in the input of pre-aged plant waxes to lakes in the lowland Neotropics (Figure 1A). Finally, $^{14}C_{wax}$ analyses were performed in soils from three locations within the Lake Chichancanab catchment (Figure 1B) to constrain the sources and transport pathways of plant waxes to lake sediments.

2. Materials and Methods

2.1 Study Areas

Lake Chichancanab is an elongate, fault-bounded lake located in the karstic interior of the Yucatan Peninsula, southeast Mexico (Figure 1). The lake spans approximately 6.5 km^2 in surface area, and has a maximum water depth of 15 m (Hodell et al., 2005). The lake catchment covers approximately 137 km^2, with low-relief, semi-deciduous tropical forest and woodland, and scattered agricultural settlements. Annual precipitation is approximately 1160 mm, with distinct dry and wet seasons (New et al., 2002; Hodell et al., 2005).

Lake Chichancanab is a closed-basin lake, with water derived from direct precipitation, runoff, and groundwater, but no surface inflows or outflows. Groundwater recharge probably comes largely from the eastern shore, where there is a fault (Perry et al., 2002). The lake is situated in carbonate bedrock with abundant evaporates marked by low permeability relative to more northerly areas in the Yucatan Peninsula (Perry et al., 2002). Sediment cores from Lake Chichancanab were intensively

studied for mineralogical and isotopic records of paleoenvironmental change. These records demonstrate marked climate variability over the past 10,000 years, including a series of intense droughts between 1200 and 850 years BP, during the Terminal Classic period of the Lowland Maya civilization (Hodell et al., 1995; Hodell et al., 2001; Hodell et al., 2005).

Surface sediments from three other lakes on the Yucatan Peninsula (Figure 1), Lake Salpeten, Punta Laguna, and Laguna Itzan, were also collected and analyzed for $^{14}C_{wax}$. These four lakes span a broad range of climate and geomorphology, providing insights into the factors that control variability of lake-sediment $\Delta^{14}C_{wax}$ in this region (Table 1). Catchment area and relief were calculated using 90-m Shuttle Radar Topography Mission (SRTM) digital elevation model datasets. Annual precipitation at each site was estimated using the Climate Research Unit high-resolution gridded climatology dataset for the years 1961-1990 (New et al., 2002).

2.2 Sediment, Soil and Plant Samples

Surface sediments from Lake Chichancanab, Lake Salpeten and Laguna Itzan were sampled from the tops of cores collected in 2004, 1999 and 1997, respectively (Breckenridge, 2000; Rosenmeier et al., 2002; Hodell et al., 2005). Sediments from Lake Chichancanab were collected at 14.7 m water depth, near the maximum depth of the lake. Sediments from Lake Salpeten were collected at 16.3 m water depth, approximately 16 meters above the deepest lake depth. Sediments from Laguna Itzan were collected in 10.1 m water depth, near the maximum lake depth. Surface sediments from Lake Punta Laguna were collected with an Ekman dredge in 2001 from the eastern basin of the lake

(Hodell et al., 2007). The sediment sample analyzed in this study comes from 16.3 m water depth, near the maximum depth of that basin. All surface sediment samples were stored in either plastic bags, or as part of sediment cores wrapped in plastic film, and were kept at 4°C from shortly after the time of collection.

Lake Chichancanab sediment cores were collected using a piston coring device along a depth transect in March, 2004 (Hodell et al., 2005). This study focuses on core CH1 7-III-04, which was collected at a water depth of 14.7 meters, near the maximum lake depth (Hodell et al., 2005). The Lake Chichancanab sediment cores were split, wrapped in plastic film and stored at 4°C from shortly after the time of collection. Within this sediment core we analyzed $\Delta^{14}C_{wax}$ in 10 horizons, and δD_{wax} in 95 additional core depths.

In December 2012, soil samples were collected from sites surrounding Lake Chichancanab (Figure 1B). Sites A and B are located in forested uplands approximately 15 and 24 m above the lake, respectively. Site C is located near the lakeshore in a low-lying area, < 1 meter above lake level, and is inundated during periods of high water level. At each site, samples were collected from a pit wall. At site A samples were collected at 5 cm, 40 cm, and 70 cm; site B samples were collected at 20 and 50 cm, and at site C samples were collected at 5, 35 and 70 cm. The 35- and 70-cm samples from locality C, however, did not contain sufficient quantities of long-chain *n*-alkanoic acids for $\Delta^{14}C_{wax}$ analysis, and were not studied further.

The δD_{wax} and $\delta^{13}C_{wax}$ values of emergent aquatic plants were analyzed to assess the possibility of their contribution to sedimentary plant waxes. We collected the most common emergent aquatic plant taxa at several lakes in southeastern Mexico and

northern Guatemala during field campaigns in 2008 and 2009 (Douglas et al., 2012). Only one emergent aquatic plant sample comes from a lake in which $^{14}C_{wax}$ was measured (Lake Salpeten), but all aquatic plant collection sites reflect similar lacustrine environments. We also measured ^{14}C in bulk leaf samples from emergent aquatic plants collected at Lake Salpeten and Laguna Yaalchak to assess the potential influence of ^{14}C-depleted carbon from lake bicarbonate.

2.3 Analytical Methods

2.3.1 Sample preparation

All sediment and soil samples were freeze-dried and solvent-extracted (ASE3000, Dionex) with an azeotrope of dichloromethane and methanol (9:1 v/v) at 150° C and 1500 psi for 5 cycles. Between 0.5 to 6 g dry sediment and between 12 and 32 g of dry soil were extracted per sample. The total lipid extract (TLE) was hydrolyzed by refluxing in 5 ml of 1 M KOH in methanol at 80°C for two hours, and then extracted with hexane and dichloromethane (2:1 v/v) to yield the neutral fraction. The pH of the residual saponified extracts was then reduced to <1 by addition of hydrochloric acid, and extracted with an azeotrope of hexane and dichloromethane (2:1 v/v) to yield the acid fraction.

Emergent aquatic plant samples were freeze-dried, cut into pieces with solvent-cleaned scissors and ultrasonically extracted with an azeotrope of dichloromethane:methanol (9:1 v/v). TLEs were separated into neutral and acid fractions using solid-phase extraction with aminopropyl sorbent (Varian Bondesil). Neutral lipids

were eluted with 8 ml of 1:9 v/v acetone:dichloromethane, and acidic lipids were eluted in 8 ml of 2% formic acid in dichloromethane.

The acid fraction of all samples was methylated using 14% boron trifluoride in methanol (70° C for 20 min). The resulting fatty acid methyl esters (FAMEs) were extracted with hexane, and purified using silica gel chromatography (eluted in 2:1 hexane:dichloromethane). Purified FAMEs were quantified relative to an external quantitative standard by GC, using a Thermo Trace 2000 GC equipped with a Restek Rxi-1ms column (60m x 0.25mm x 0.25μm), a pressure- and temperature-variable (PTV) injector and a flame ionization device (FID) with He as the carrier gas.

2.3.2 Compound-specific radiocarbon analyses

Long-carbon-chain-length FAMEs were isolated using a Preparative Capillary Gas Chromatography (PCGC) system at either the Woods Hole Oceanographic Institution Department of Marine Chemistry and Geochemistry or the National Ocean Sciences Accelerator Mass Spectrometry (NOSAMS) Facility. These systems consist of an Agilent gas chromatograph-flame ionization detector (GC-FID) coupled to a Gerstel Preparative Fraction Collector, and we applied the method described in Eglinton et al. (1996). Individual FAMEs were not sufficiently abundant for $\Delta^{14}C$ analysis, so we combined four long-chain *n*-alkanoic acid homologs (C_{26}, C_{28}, C_{30}, and C_{32}), where C_x indicates the carbon-chain length of the original fatty acid. Long-chain FAMES were collected in a chilled, pre-combusted glass trap. One sample (CH170-172) was split and isolated at different times to assess the repeatability of PCGC compound isolation. A split from all but one sample was reserved, prior to PCGC isolation, for gas chromatography-

isotope ratio mass spectrometry (GC-IRMS) analysis. Isolated FAME fractions were quantified and checked for purity by GC-FID, and contamination from column bleed was removed using silica gel column chromatography with dichloromethane as the eluent. The samples were transferred to pre-combusted quartz tubes and all solvent was evaporated under nitrogen. Pre-combusted cupric oxide was added to the tubes, which were then flame-sealed under vacuum and combusted at 850°C for five hours. The resulting CO_2 was quantified and purified on a vacuum line, and then reduced to graphite and analyzed for radiocarbon content at the NOSAMS facility. A split of sample CO_2 from most samples was measured at NOSAMS for $\delta^{13}C$ values. These $\delta^{13}C$ values were compared with GC-IRMS $\delta^{13}C$ measurements to assess for contamination from extraneous carbon.

Compound-specific radiocarbon results were corrected for procedural blanks by accounting for the blank contribution determined using the same analytical protocol and equipment. The blank contribution determined for the WHOI Marine Chemistry and Geochemistry PCGC system is 1.8 ± 0.9 µg of C with an Fm of 0.44 ± 0.10 (Galy and Eglinton, 2011), whereas the blank contribution determined for the NOSAMS PCGC system is 1.4 ± 1.2 µg of C with an Fm of 0.64 ± 0.20. The magnitude of the blank correction varies between samples, depending on the amount of carbon analyzed.

2.3.3 Compound-specific stable isotope analyses

Isotopic analyses for individual FAMEs were carried out by GC-IRMS. Measurements were performed at the Yale University Earth System Center for Stable Isotopic Studies using a Thermo Trace2000 GC equipped with an SGE SolGel-1ms

column (60m x 0.25mm x 0.25μm) and a PTV injector coupled to a Finnigan MAT 253 stable isotope mass spectrometer and a Finnigan GC combustion III interface. The H_3^+ was measured daily prior to δD analysis, with a mean value for the measurement periods of 15.6 ±0.3 (1σ). An external FAME isotope standard (Mix F8, Indiana University Biogeochemical Laboratories) and an internal laboratory isotope standard, measured after every four to six sample analyses, were used to standardize and normalize sample isotope values. The precision of the standard analyses was ≤ ±5‰ for δD analyses and ≤ ±0.5‰ for $\delta^{13}C$ analyses. Most samples were run in duplicate or triplicate for both hydrogen and carbon isotope analysis, and the reported isotope ratio values are averages of replicate runs. Insufficient abundances for some long-chain FAME samples prevented replicate δD analyses.

FAME $\Delta^{14}C$, $\delta^{13}C$, and δD values were corrected for the isotopic composition of the methyl group added during esterification. A phthalic acid standard of known isotopic composition (acquired from Indiana University Biogeochemical Laboratories) was methylated in the same manner as the samples and used to calculate the stable isotopic compositions of the added methyl carbon and hydrogen. In addition, a sample of the methanol used for esterification was analyzed for $\Delta^{14}C$ at NOSAMS and was found to contain no measureable ^{14}C. The isotopic correction for $\delta^{13}C$ and $\Delta^{14}C$ was achieved using the following equation:

$$\delta_{n-acid} = \frac{\left[(n+1)\delta_{FAME}\right] - \delta_{methanol}}{n} \qquad \text{(Equation 1)}$$

where $\delta_{n\text{-acid}}$, δ_{FAME}, and $\delta_{Methanol}$ are the isotopic value of the fatty acid, the measured fatty acid methyl ester, and the added methyl carbon respectively, and *n* is the number of carbon atoms in the original fatty acid. Because compound-specific $\Delta^{14}C$ measurements were conducted on a set of combined *n*-alkanoic acids (*n*-C_{26}, *n*-C_{28}, *n*-C_{30}, and *n*-C_{32}), we computed the corrected value using the average chain length of the combined molecules, determined by GC-FID analyses. The isotopic correction for δD measurements was achieved using the equation:

$$\delta_{n-acid} = \frac{\left[(n+1)\delta_{FAME}\right] - \delta_{methanol}}{n} \quad \text{(Equation 2)}$$

where *n* is the number of hydrogen atoms in the fatty acid.

2.4. Construction of age-depth models

An age-depth model for Lake Chichancanab plant-wax radiocarbon ages was developed using the 'Classical age-depth modeling' (CLAM) software (version 2.2) in R (Blaauw, 2010). We applied a smoothing spline fit to dated horizons, with a smoothing parameter of 0.3, to determine a plant-wax-specific age model, hereafter referred to as the 'PW age model'. 95% confidence intervals were calculated by analyzing the distribution of 1000 randomly generated age models (Blaauw, 2010). The 'best' age model was determined by calculating the mean age of all model iterations at each depth in the core. All radiocarbon ages were calibrated using the INTcal13 calibration curve (Reimer et al., 2013).

We also recalculated the sediment core age model for core CH1 07-III-04 based on terrigenous macrofossil ages (Hodell et al., 2005) using CLAM. The terrigenous

macrofossil radiocarbon ages used to define this age model are not derived from a single core, but instead are a compilation of ^{14}C ages from several cores projected onto core CH1 07-III-04 based on correlations in sediment density and color profiles (Hodell et al., 2005). In the case of the age-depth model developed using terrigenous macrofossil ages, referred to as the 'TM age model', we applied a 2nd order polynomial, as was done previously for this core (Hodell et al., 2005).

2.5 Numerical Simulations of Plant-wax Age Distributions

$^{14}C_{wax}$ data indicate the mean age of plant waxes in a given stratigraphic horizon, but do not constrain the distribution of plant wax ages around that mean, which is an important consideration for interpreting plant-wax stable isotope records. We designed a set of numerical modeling exercises to simulate the effects of different plant-wax age distributions on sediment δD_{wax} records. These modeling exercises entailed passing a plant-wax age distribution 'filter' through both (1) a hypothetical synthetic record of past climate variability and (2) an independently dated proxy record of past climate variability based on gastropod $\delta^{18}O$ values from Lake Chichancanab (Hodell et al., 1995). The goals of these simulations were to: (1) observe how different plant-wax age distributions distort primary paleoclimate signals; and (2) to constrain which age distributions were most consistent with the observed $\Delta^{14}C_{wax}$ and δD_{wax} data from Lake Chichancanab.

For these simulations, we assume that overall plant-wax age distribution (*A*) is bimodal, with a decadal (*D*) and a millennial (*M*) age component (Drenzek, 2007). *A* is a linear combination of these two components:

$$A = f_D D + f_M M \qquad \text{(Equation 3)}$$

where f_D and f_M are the fraction of plant waxes derived from the decadal and millennial pools, respectively. Each component is assumed to be distributed normally, and truncated at the time of sediment deposition (time = 0). The truncated normal distribution is expressed as follows (Barr and Sherrill, 1999):

$$f(x) = \frac{1}{\sqrt{2\pi}\left[1-\Phi\left(-\frac{\mu}{\sigma}\right)\right]}\exp\left(-\frac{(x-\mu)^2}{2\sigma^2}\right) \quad \text{(Equation 4)}$$

where μ and σ define the mean and standard deviation of the corresponding non-truncated normal distribution and Φ is the cumulative distribution function of a standard normal distribution.

Based on Equations 3 and 4, A is defined by six unknown parameters: f_D, μ_D, σ_D, f_M, μ_M, and σ_M. μ_D and μ_M are equivalent to the mean catchment residence time of plant waxes in decadal and millennial cycling pools, respectively. σ_D and σ_M indicate the age variance of plant waxes in the decadal and millennial pools, respectively. Data and assumptions allow us to reduce this to two free parameters. First, we assume that the decadal parameters μ_D and σ_D are fixed at 15 and 10 years, respectively. The assumed value for μ_D was selected as the mean of previous estimates of the mean age of the decadal pool of plant waxes from marine sediments in the Cariaco Basin, north of Venezuela (10 years) and the Saanich Inlet, near Vancouver Island, British Columbia, Canada (20 years) (Drenzek, 2007). Although there are few constraints on σ_D, 10 years is a reasonable estimate for the age variance of a decadally cycled pool of plant waxes.

Second, A, D and M are probability distributions and each integrate to 1, and therefore $f_D + f_M = 1$. Third, estimated values of the mean soil residence time of plant

waxes (MRT_{wax}) (*see section 3.1.4*), derived from the age difference between the PW and TM age models, reflects the mean age of plant waxes in a stratigraphic horizon at the time of sediment deposition and are equivalent to the weighted mean of A ($\overline{A}$). Therefore we can use estimates of MRT_{wax} to constrain one of the remaining parameters, using the following relationship:

$$MRT_{wax} = \overline{A} = (1 - f_M)\overline{D} + f_M \overline{M} \quad \text{(Equation 5)}$$

Combining equation 4 with equation 5 gives a nonlinear equation to be solved for the constrained parameter (either f_M, μ_M, or σ_M):

$$\overline{A} = (1 - f_M)\overline{D} + f_M \left(\mu_M + \frac{\sigma_M}{\sqrt{2\pi\left(1 - \Phi\left(\frac{-\mu_M}{\sigma_M}\right)\right)}} \exp\left(\frac{-\mu_M^2}{2\sigma_M^2}\right) \right) \quad \text{(Equation 6)}$$

where $\overline{D}$ is calculated from μ_D and σ_D. Thus we have two free parameters, which can be any combination of f_M, μ_M, or σ_M.

It is important to note that the mean plant-wax age, $\overline{A}$, is defined for a single stratigraphic horizon, and changes significantly throughout the Lake Chichancanab sediment core (*see section 3.1.4*). This means that in simulations of Lake Chichancanab plant-wax age distributions the constrained parameter is not constant.

To invert for an optimal age distribution, we assert that the best solution is that which minimizes the misfit between two time-series: (1) the observed Lake Chichancanab δD_{wax} record fit to the TM age model and (2) an independently dated reference climate proxy record (δ_{ref}) that has been filtered through that age distribution

(δ_{synth}). For δD_{wax}, we applied the mean values of long-chain *n*-alkanoic acid homologs (*see section 3.2.1*). We selected the Lake Chichancanab gastropod $\delta^{18}O$ record (Hodell et al., 1995) as the reference climate record (δ_{ref}), for two reasons: (1) it is from the same lake and should record climate changes similar to the δD_{wax} record; and (2) it is the longest available record from the region, extending back >7000 years, allowing us to model age distributions with relatively large values for μ_M or σ_M. The gastropod $\delta^{18}O$ record is not a perfect representation of δD_{wax} variability. However, both climate proxies are largely controlled by the same processes, namely the relation between the amount of precipitation and the intensity of evapotranspiration (Hodell et al., 1995; Douglas et al., 2012), and therefore are likely to produce similar records, at least on centennial and longer timescales.

To perform the inverse analysis, we generate δ_{synth} records for given values of the two free parameters by (1) solving for the value of the constrained parameter that satisfies the data $\overline{A}(t)$ at each time point, (2) computing the resulting age distribution, and (3) computing a δ_{synth} value at each time point using the following relationship:

$$\delta_{synth}(t) = \sum_{i=t}^{n} \left[\left(\delta_{ref}(i) \right) \left(A(i) \right) \right] \qquad \text{(Equation 7)}$$

where $\delta_{synth}(t)$ is the value of the synthetic record at a time point t, $\delta_{ref}(i)$ is the value of the reference curve at a time i that precedes time t, $A(i)$ is the probability density of the plant-wax age distribution at time i, and n is the oldest time point in the δ_{ref} record (~7000 years).

We quantify the misfit between the δ_{synth} and δD_{wax} record for each set of free parameters tested, and search the parameter space for the minimum misfit using the Neighborhood Algorithm (Sambridge, 1999). We performed two sets of inverse analyses that included either (1) f_M and σ_M, or (2) μ_M and σ_M as the two free parameters. The parameter space analyzed ranges from 0 to 1 for f_M, 0 to 2000 for σ_M, and 0 to 5000 for μ_M. Misfits were quantified using the metric 1-r, where r is the Pearson's product-moment correlation coefficient.

In order for the δ_{ref} record to have values that are comparable to the δD_{wax} record, we transformed the original gastropod $\delta^{18}O$ values using the following equation

$$\delta_{ref} = k\left(\delta^{18}O - \overline{\delta^{18}O}\right) - \overline{\delta D_{obs}} \qquad \text{(Equation 8)}$$

where $\overline{\delta^{18}O}$ is the mean of the gastropod $\delta^{18}O$ record (1.8‰), k is a scaling factor (from 8 to 16), and $\overline{\delta D_{obs}}$ is the mean of the δD_{wax} record (-120‰). We primarily apply a value of k (12) that is 1.5 times greater than the scaling factor between $\delta^{18}O$ values and δD values on the global meteoric water line (i.e., 8) (Rozanski et al., 1993), because in this region δD_{wax} values are strongly influenced by evapotranspiration, which amplifies changes in δD_{wax} caused by variability in the δD composition of precipitation (Douglas et al., 2012). This choice is also based on the observation that the range of observed δD_{wax} values (45‰) is 11.5 times the observed variability in the gastropod $\delta^{18}O$ record (3.9‰), despite possible attenuation as a consequence of filtering through plant-wax age distributions (*see section 3.2.1*). We also performed sensitivity tests using values of 8 and 16 for k.

Because of age uncertainty in both the TM and PW age models for the Lake Chichancanab core, it is highly unlikely that our inverse model results can account for decadal variability in the Lake Chichancanab δD_{wax} record. Therefore, the primary goal of this exercise was to determine which age distributions are most consistent with the centennial- to millennial-scale variability in the δD_{wax} record. Decadal variability in the δD_{wax} record could interfere with the ability of the model to find a best-fit solution. To address this possible interference, we compared the model-generated δ_{synth} records with a set of δD_{wax} records with different degrees of smoothing. These records include an unsmoothed record, a three-point running average, a five-point running average, and a record with the δD_{wax} data binned into 100-year intervals. We did not smooth the original gastropod $\delta^{18}O$ record (δ_{ef}), as the process of filtering this record through the plant-wax age distribution (equation 7) smooths the resulting δ_{synth} record.

3. Results

3.1 Compound-specific radiocarbon results

3.1.1 Lake surface sediment $^{14}C_{wax}$

$\Delta^{14}C_{wax}$ in the studied core top sediments ranges from -8 to -69 ‰, corresponding to ^{14}C ages between 20 and 520 years BP, respectively (Figure 2; Table 2). These data indicate that the majority of plant waxes in these uppermost lake sediments predate 1950, because their ages do not reflect a substantial "post-bomb," positive $\Delta^{14}C$ signal. $\Delta^{14}C_{wax}$ varies widely across southeastern Mexico and northern Guatemala, possibly because of environmental differences between these lake catchments. $\Delta^{14}C_{wax}$ in surface sediments is

generally higher (i.e., younger radiocarbon ages) in lakes with greater mean annual precipitation and smaller catchment areas (Figure 2). In the four studied lakes, there is no apparent relationship between $\Delta^{14}C_{wax}$ and topographic relief in the lake catchment.

3.1.2 Lake Chichancanab catchment soil $^{14}C_{wax}$

Soil $\Delta^{14}C_{wax}$ ranges from 120 to -44‰ (Table 2), corresponding to ^{14}C ages ranging from post-1950 to 300 years BP. Both samples from topsoil horizons (5 cm) contain predominantly modern carbon, and at the two sites with depth profiles, there is a trend of increasing age with depth in the soil (Figure 3).

3.1.3 Lake Chichancanab sediment core $^{14}C_{wax}$

Plant-wax ages increase with depth in the lake core (Figure 4), with two prominent exceptions that are markedly older than other sediment core samples. These two samples were likely contaminated with extraneous carbon either from column bleed or incompletely evaporated solvent, as indicated by a relatively large deviation between the $\delta^{13}C$ value measured in sample CO_2 and by GC-IRMS (Eglinton et al., 1996) (Table 3), and by a large difference in the amount of isolated sample quantified as CO_2 and via GC-FID. Accordingly, these two radiocarbon ages were excluded from subsequent analyses and interpretation. Results from repeat isolations of sample from 170-172 cm are remarkably close in age (Table 3), indicating that the PCGC isolation techniques applied in this study yield reproducible compound-specific radiocarbon data.

3.1.4 Lake Chichancanab plant wax (PW) and terrigenous macrofossil (TM) age models

The 'best' PW age model extends from 3692 to 557 years BP (Figure 4a). The 95% confidence intervals range from 142 to 313 years, with an average confidence interval of 231 years. Of 1000 age model iterations, 13% resulted in age reversals and were discarded. The 'best' TM age model extends from 2404 to -58 years BP (Figure 4a). The 95% confidence intervals range from 26 to 306 years, with an average confidence interval of 108 years. The PW-age model is consistently older than the TM age model at all core depths, and at no point in the core do the confidence intervals of the two age models overlap (Figure 4a).

Assuming that the majority of plant waxes found in the lake sediment came from soils surrounding the lake (*see sections 4.3 and 4.4*), age offsets between the PW and TM age models indicate the approximate mean residence time of plant waxes (MRT_{wax}) in catchment soils, which in the Lake Chichancanab sediment core varies from ~350 to 1200 years (Figure 4b, Table 3).

3.2 Compound-specific stable isotope results

3.2.1 Lake Chichancanab δD_{wax} values

We analyzed δD values of *n*-C_{26}, *n*-C_{28}, and *n*-C_{30} alkanoic acids in the Lake Chichancanab sediment core (Supplemental Table S1). Although *n*-C_{32} was included in samples for $^{14}C_{wax}$ measurements, its abundance was often too low for D/H analysis.

We found consistent δD differences among *n*-C_{26}, *n*-C_{28}, and *n*-C_{30}, with *n*-C_{28} the most D-enriched (mean δD: 100±14‰ 1σ), *n*-C_{30} intermediate in δD composition (mean δD:125±10‰ 1σ), and *n*-C_{26} the most D-depleted (mean δD: 135±12‰ 1σ). This inter-homolog δD variability in the Chichancanab core is similar to variability observed in lake

surface sediments from this region (Douglas et al., 2012), although on average, variability in Lake Chichancanab sediments is larger than that in the other regional lakes. The inter-homolog isotopic variability in the sediment core also differs from that in catchment soil samples (Supplemental Table S2), which display increasing D enrichment in the higher-carbon-number homologs. Studies of D/H composition of *n*-alkanoic acids in leaves from East Asia show large inter-homolog variability in some taxa, without a consistent pattern between plants (Chikaraishi et al., 2004). It is also possible that some sedimentary plant waxes derive from emergent aquatic plants (*see Section 4.3*). Inter-homolog variability in emergent aquatic plant samples from our study area is variable, with no consistent trend (Supplemental Table S3). Inter-homolog δD differences observed in the Lake Chichancanab core potentially result from different plant sources, although this hypothesis requires further testing.

For comparison with other paleoclimate records, we primarily focus on the mean δD value (δD_{mean}) of *n*-C_{26}, *n*-C_{28}, and *n*-C_{30} homologs, for two reasons. First, $\Delta^{14}C_{wax}$ measurements were performed on a combined set of long-chain *n*-alkanoic acids, and it is appropriate to compare these data with a mean homolog δD value. Second, these homologs likely derive from different source plants, with potential differences in their D/H response to hydroclimate change, thus δD_{mean} provides the most general indication of past climate change. We do not employ abundance-weighted mean δD values because they could vary in response to vegetation changes that affect the relative abundance of individual homologs.

The Lake Chichancanab δD_{wax} record indicates substantial hydroclimate variability in the northern Yucatan Peninsula during the late Holocene (Figure 5a,b), a

finding that is consistent with other paleoclimate records from the region (Figure 5c,d,e,f) (Hodell et al., 1995; Curtis et al., 1996; Hodell et al., 2001; Hodell et al., 2005; Medina-Elizalde et al., 2010; Kennett et al., 2012; Medina-Elizalde and Rohling, 2012). The overall amplitude of δD_{wax} variability is relatively large (40‰), and there is substantial high-frequency δD_{wax} fluctuation (~20‰) on decadal time scales (Figure 5a,b).

Application of the PW age model shifts the age of δD_{wax} values back in time relative to the TM age model (Figure 5a,b), producing a pattern more consistent with other climate proxy records from the region (*see section 4.5*).

3.2.2 Lake Chichancanab catchment soils δD_{wax} and $\delta^{13}C_{wax}$ values

Lake Chichancanab catchment soil $\delta^{13}C_{wax}$ values, reported as means of *n*-C_{26}, *n*-C_{28}, *n*-C_{30}, and *n*-C_{32} homologs, span a wide range from -25.1 to -32.8‰ (Supplemental Table S2). The sample from Site C, which is dominated by grasses, has a highly ^{13}C-enriched value, suggesting significant input from C_4 plants, whereas the samples from Sites A and B, located in forests, are more ^{13}C-depleted, consistent with the surrounding C_3 flora (Supplemental Table S2). The overall range in $\delta^{13}C_{wax}$ values from catchment soils encompasses the range of $\delta^{13}C_{wax}$ values from Lake Chichancanab sediment core samples (Figure 6a).

In contrast to $\delta^{13}C_{wax}$ values, δD_{wax} values from Lake Chichancanab catchment soils span a relatively narrow range, from -149 to -133‰. Soil δD_{wax} values are relatively D-depleted compared to the sediment core, although some values overlap, including the δD value for the lake surface sediment (Figure 6b).

3.4 Model Results

3.4.1 Inverse modeling of Lake Chichancanab plant-wax age distributions

Inverse model runs with a range of scaling factors for the $\delta^{18}O$ reference curve (k) and different degrees of smoothing for the δD_{wax} record, return similar results (Table 4), with only minor differences in the best-fit model parameters and the degree of misfit between the δD_{wax} and δ_{synth} records. In runs where f_M and σ_M are the free parameters, the best-fit model values are centered around 0.83 for f_M and 79 years for σ_M (Figure 7a; Table 4). δ_{synth} records with low values for σ_M (< 200 years) and with f_M values as great as 1 also have relatively good fits (i.e. $r > 0.6$ in Figure 7a). In simulations where μ_M and σ_M are the free parameters, the best-fit model values range between 1342 and 1345 years for μ_M, and between 5 to 18 years for σ_M (Figure 7b, Table 4). In these models, the best-fit values are located in a narrow range near the lower limit of possible μ_M values with very low values for σ_M (Figure 7b), suggesting that allowing μ_M to vary to lower values at some points in the record would improve the model fit. For every given set of model conditions, models in which f_M and σ_M are the free parameters provide a better fit than when μ_M and σ_M are the free parameters (Figure 7; Table 4).

3.4.2 Forward modeling of plant-wax age distribution effects on a synthetic climate record

To clarify the effects of different plant-wax age distributions on sediment δD_{wax} records, we filtered a simplified synthetic climate record through three hypothetical age

distributions (Figure 8). The synthetic climate record contains both millennial-scale and decadal-scale variability, and is broadly similar to the record of the Terminal Classic Drought observed in the Maya Lowlands (Figure 5).

In Scenario 1, with a relatively low f_M and a high σ_M, millennial-scale variability in the filtered record is split between the decadal and millennial plant-wax populations, and this variability is attenuated to 42% and 52% of the original signal, respectively. Decadal variability in the filtered record is primarily imparted by the decadal plant waxes and is attenuated to roughly 30% of the original signal. In this scenario, neither the TM nor PW age model would provide a clear indication of the original climate variability (Figure 8b,c) and our inverse model results indicate that the $\Delta^{14}C$ and δD_{wax} data from Lake Chichancanab are not consistent with this scenario (Figure 7a).

In Scenario 2, with intermediate values for σ_M and f_M, most of the millennial-scale variability is transmitted by millennial plant waxes, and is attenuated to 80% of the original signal. Some millennial-scale variability is also transmitted through the decadal pool. The decadal climate signal is still primarily transmitted by decadal plant waxes, and is attenuated to 23% of the original signal. In this scenario, the plant-wax age model provides an approximate indication of millennial-scale climate variability, although the onset, peak and termination of the climate event would be temporally offset and the amplitude significantly attenuated (Figure 8b). Our inverse model results suggest that this scenario is consistent with the Lake Chichancanab $\Delta^{14}C$ and δD_{wax} data, as its f_M and σ_M values fall near the range of best-fit solutions (Figure 7a)

In Scenario 3, with very high values for f_M and very low values for σ_M, both the decadal and millennial climate signals are primarily imparted by millennial plant waxes,

with minimal additional variance from the decadal plant waxes. The millennial climate signal is only attenuated slightly, to 95% of the original signal, and the decadal climate signal is attenuated to 63% of its original signal. In this scenario, the PW age model provides a reasonable record of both the millennial and the decadal climate variability. While the values for f_M and σ_M in this scenario do not overlap the best-fit solutions in our inverse model results (Figure 7a), we cannot exclude it as being representative of the Lake Chichancanab δD_{wax} record because (1) these parameters still result in a relatively good fit (Figure 7a) and (2) the inability of the inverse model to account for high-frequency variability in the δD_{wax} record potentially biases its results against solutions with higher-amplitude decadal climate variability.

4. Discussion

4.1 $^{14}C_{wax}$ variability in lake surface sediments

The four lakes evaluated in this study are spread across a wide geographic area in southeastern Mexico and northern Guatemala, and all four possess pre-aged plant waxes in their surface sediments. This observation is consistent with $^{14}C_{wax}$ data from marginal marine sediments, which indicate the widespread input of pre-aged plant waxes (Smittenberg et al., 2004; Uchida et al., 2005; Drenzek et al., 2007; Drenzek et al., 2009; Kusch et al., 2010; Feng et al., 2012). However, the range of plant-wax ages in these lake surface sediments (20 to 520 ^{14}C years BP) are younger than most plant-wax ages from marine sediments (820 to 5600 ^{14}C years BP). This difference could be a consequence of longer transit times for plant waxes to reach marine sediments, or longer time scales of sediment focusing and organic carbon advection in marine sedimentary

basins. Alternatively, younger plant-wax ages in this study reflect faster turnover of plant waxes in tropical climates, as most of the previous studies of $^{14}C_{wax}$ are derived from mid- to high-latitude settings.

The age of plant waxes in marine and lacustrine sediments is potentially controlled by a number of environmental variables, including soil characteristics, environmental conditions, and pathways of plant-wax transport. For example, $^{14}C_{wax}$ data from modern Black Sea sediments collected in different drainage basins indicate that catchment area, relief, and precipitation amount can all influence the mean age of sedimentary plant waxes (Kusch et al., 2010). $\Delta^{14}C_{wax}$ values from our studied lakes increase with higher precipitation and decrease with larger catchment area (Figure 2).

Land use varies widely between our sites and could be an additional control on $\Delta^{14}C_{wax}$ values. Land use is more intense in the catchments of Guatemalan Lakes Salpeten and Itzan, than in the catchments of Mexican Lakes Chichancanab and Punta Laguna. If more intense land use contributed to faster turnover and increased leaching of organic matter from soils, this could explain the higher $\Delta^{14}C_{wax}$ values in Lakes Salpeten and Itzan. A decrease in $\Delta^{14}C_{wax}$ related to land use is consistent with evidence for decreased storage of carbon in deep soil layers following deforestation in a Costa Rican forest (Veldkamp et al., 2003). Past land use change in the Chichancanab catchment, where there is evidence for ancient agriculture (Leyden, 2002), potentially explains variability of MRT_{wax} in the sediment core (Figure 4b).

4.2 $^{14}C_{wax}$ variability in Lake Chichancanab catchment soils

Currently, there are very few $^{14}C_{wax}$ data for soils. The only published study evaluated a temperate soil from Japan, sampled from 20 to 30 cm depth in a forested setting. The soil contained long-chain *n*-alkanoic acids (C_{26} to C_{30}) with $\Delta^{14}C$ signatures that indicated a substantial fraction of post-bomb carbon (17 to 79‰) (Matsumoto et al., 2007). Our results demonstrate that pre-modern plant-wax ages occur in some tropical forest soils (Figure 3). In the two soil profiles studied, $\Delta^{14}C_{wax}$ decreased with depth, consistent with evidence for ^{14}C-depletion with depth for organic carbon in the high-density (mineral-associated) fraction of tropical soils from Brazil and Hawaii (Trumbore et al., 1995; Torn et al., 1997; Trumbore, 2000).

These results suggest that lipids mobilized from the deeper horizons of the catchment soils are the likely source of aged plant waxes in Lake Chichancanab sediments. Ages of soil plant waxes are not as old as those in lake surface-sediments. The base of the soils, particularly on the east side of the lake, was not adequately sampled, however, and the oldest soil plant-waxes were likely not recovered.

Hydrogeological studies suggest that groundwater entering Lake Chichancanab is primarily transported through a fault on the east side of the lake, where our results indicate soil plant-waxes are older for a given soil depth (Figure 3). This suggests that deeper soil horizons, or deep soil-horizons in other parts of the lake catchment, are the source of plant waxes for the lake surface-sediments, with flux from the soil base into the karst geology (*see section 4.4*). If a linear decrease in $\Delta^{14}C_{wax}$ with soil depth is assumed, our results predict that the predominant source of plant waxes to lake surface sediments is from soils approximately 80 to 103 cm below the land surface (Figure 3).

An additional consideration is the possibility that the oldest plant waxes in soil reservoirs are mineral-bound and that these plant waxes are preferentially preserved in lake sediments (Vonk et al., 2010). We did not attempt to isolate mineral-bound plant waxes in our analysis of soil samples, but this could be an important direction for future research.

4.3 Other possible sources of aged plant waxes

There are several possible ways to explain the pre-aged signal in the surface sediments of Lake Chichancanab. Whereas our evidence supports the presence of aged plant waxes in Lake Chichancanab catchment soils, the appearance of pre-aged plant waxes in lake sediments could potentially derive from *in situ* aquatic plant production or from the redistribution of sediments within the lake.

4.3.1 ^{14}C-depleted aquatic plants

Some aquatic plants incorporate aqueous bicarbonate during carbon fixation (Aravena et al., 1992). Lake Chichancanab is situated in Eocene- to Pliocene-age carbonate and evaporite bedrock (Perry et al., 2002; Bauer-Gottwein et al., 2011), and bicarbonate in the lake waters is ^{14}C-depleted relative to the atmosphere (Hodell et al., 1995). ^{14}C ages of lacustrine shells indicate a modern bicarbonate ^{14}C age of ~1200 years (Hodell et al., 1995), although this "hard-water error" effect appears to have varied considerably during the past 9000 years based on the comparison of carbonate and

terrigenous macrofossil ^{14}C ages. If modern aquatic plants incorporate 'dead' carbon and produce waxes similar to those in the surrounding flora, these compounds would appear pre-aged despite an autochthonous origin and rapid transport to underlying sediments. This scenario is unlikely in Lake Chichancanab for several reasons. First, although submerged aquatic plants are more likely to incorporate carbon from ^{14}C-depleted bicarbonate, they are unlikely to impart a strong ^{14}C-depleted signature to sedimentary long-chain *n*-alkyl lipids because they do not typically produce large amounts of long-chain *n*-alkanoic acids (Ficken et al., 2000).

Second, the stable isotopic composition of emergent aquatic plants from lakes in the region suggests they are not the source of sedimentary, long-chain fatty acids. Emergent aquatic plant $\delta^{13}C_{wax}$ values range from -34.7 to -39.8‰, and δD_{wax} values range from -132 to -192‰ (Supplemental Table S3). The aquatic plant samples are all significantly ^{13}C-depleted relative to the sediment samples analyzed for $^{14}C_{wax}$ (Figure 6a) and, with one exception, are also significantly D-depleted relative to sedimentary plant waxes from Lake Chichancanab (Figure 6b). Instead, the stable isotopic composition of plant waxes in Lake Chichancanab sediments echo values observed from soils in the surrounding catchment and other areas in the northern Yucatan Peninsula (Figure 6). Given Lake Chichancanab's bicarbonate reservoir age of 1200 years BP in surface sediments, a $^{14}C_{wax}$ age of 520 years would require ~45% of plant waxes to come from aquatic plants that derive 100% of their carbon from aged lake bicarbonate — an unlikely scenario given the stable isotopic relationships presented above. Furthermore, measurements of bulk $\Delta^{14}C$ values in emergent aquatic plant leaves from two lakes with ^{14}C-depleted bicarbonate in the Maya Lowlands (Lake Salpeten, +39±3 ‰; Laguna

Yaalchak, +52±3 ‰) indicate these plants are composed of predominantly modern carbon from the atmosphere, and do not incorporate significant amounts of ^{14}C-depleted bicarbonate from the lake water, implying that they do not constitute a source of pre-aged plant waxes to sediments.

4.3.2 Redistribution of lake sediments

Vertical (bioturbation) or lateral (resuspension and advection) mixing could potentially introduce organic carbon from older lake sediments, which would account for aged plant waxes in Lake Chichancanab sediments without invoking input from surrounding soils. However, vertical mixing is an unlikely explanation. Whereas there are no water-column temperature or oxygen concentration data for Lake Chichancanab, lakes in similar environments in the Yucatan (Hodell et al., 2007) and Guatemala are thermally stratified throughout much of the year (Deevey et al., 1980) with low oxygen at the sediment-water interface. Similar oxygen-poor conditions likely exist at Lake Chichancanab, limiting the depth of bioturbation. Lake Chichancanab has a relatively high sedimentation rate, averaging 0.89 mm/yr in the sediment core studied here (Hodell et al., 2005). Assuming continuous modern-age plant wax deposition, to generate a mean plant-wax surface sediment age of 520 ^{14}C years BP would require homogenizing at least the top 60 cm of sediment. There is no evidence of such deep mixing in the mineralogical and carbonate isotope records (Hodell et al., 1995; 2001; 2005), nor in the pollen profile (Leyden 2002) from this lake.

Resuspension of old plant waxes from shallow lake sediments could occur as a consequence of sediment focusing, or the redistribution of sediment from shallow to

deeper areas of the lake. However, tracer studies of radionuclides in lakes indicate that sediment focusing redistributes lake sediments on time scales of 10 to 20 years (Wieland et al., 1991; Crusius and Anderson, 1995), far shorter than the values of MRT_{wax} observed in the Lake Chichancanab sediment core (Figure 4b). It is highly unlikely that timescales of sediment focusing would be significantly longer at Lake Chichancanab, which is both relatively shallow (15 m depth) and narrow in cross section (700 m at its widest), limiting the potential distance of sediment transport within the lake. Furthermore, sediment focusing in lake sediments is associated with significant temporal smoothing of sediment core geochemical profiles (Crusius and Anderson, 1995). If sediment focusing were responsible for the presence of pre-aged plant waxes in Lake Chichancanab, sediments it would likely be associated with centennial-scale smoothing of the δD_{wax} record. Such smoothing is not consistent with the high-frequency variability in this record (Figure 5a,b) and the lack of a good fit for plant-wax age distributions with high σ_M values in our inverse modeling simulations (Figure 7).

4.4 Mode of transport of plant waxes from soils

Given the age and stable isotope composition of soil plant waxes, as well as the catchment and lake hydrology, we conclude that pre-aged plant waxes in Lake Chichancanab sediments derive predominantly from catchment soils. There are two likely modes of transport for aged plant waxes from soils to lake sediments: (A) overland transport in eroded soil, and (B) subsurface transport as a component of dissolved or colloidal organic carbon.

Lake Chichancanab receives hydrologic inputs primarily through direct precipitation and groundwater infiltration (Hodell et al., 2005), with groundwater input concentrated on the eastern slope of the basin (Perry et al., 2002). There are no perennial streams feeding Lake Chichancanab and there is no evidence for substantial contributions of eroded soil in lake sediments, as sediments are very rich in organic carbon and do not contain large proportions of clay or detrital minerals (Hodell et al., 1995; Hodell et al., 2005). Notably, our soil $^{14}C_{wax}$ data suggest plant waxes in topsoils are predominantly modern in age (Figure 3). In this relatively low-relief catchment (Figure 1b), it is unlikely that surface exposure of subsoil horizons is significant. If plant waxes from subsoil horizons were eroded by surface flow, transported plant waxes would be sampled from a wide range of soil horizons, which would lead to significant mixing of waxes of different ages.

In this karst environment, most precipitation moves quickly through the permeable vadose zone (Perry et al., 2002), and, despite their relatively hydrophobic nature, long-chain *n*-alkanoic acids and other lipids are known to be transported through soils (Colina-Tejada et al., 1996; Nierop and Buurman, 1998; Bull et al., 2000; Naafs et al., 2004). The presence of dissolved organic matter has been shown to generally increase the solubility of hydrophobic organic compounds in aquatic and soil systems (Hassett and Anderson, 1979; Bengtsson et al., 1987), and many hydrophobic compounds are transported through soils via colloidal dispersion (Ouyang et al., 1996). The residence time of plant waxes transported through subsurface soils is likely controlled by sorption and desorption processes. Lipids are readily sorbed to soil minerals and natural organic matter and compete with other hydrophobic organic compounds for sorption sites (Kohl

and Rice, 1999; Ding and Rice, 2011). The controls on the sorption and desorption of hydrophobic organic molecules in soils are not well constrained, but some research suggests that possible important factors include cycles of wetting and drying (Pignatello, 2012) and soil age (Waldner et al., 2012).

Comparisons of $\Delta^{14}C_{wax}$ values from Lake Chichancanab surface sediments and catchment-soil profiles suggest that relatively deep subsoil horizons (> 50 cm) are the source of pre-aged plant waxes in these lake sediments (Figure 3). However, given the very limited data currently available constraining the transport of plant waxes in terrestrial ecosystems, the exact pathways that transfer this pre-aged plant wax signal to Lake Chichancanab sediments remain to be determined.

4.5 Effects of pre-aged plant waxes on interpretation of the Lake Chichancanab δD_{wax} record

δD_{wax} values record the isotopic composition of plant water at the time of lipid biosynthesis (Feakins and Sessions, 2010; Kahmen et al., 2012; Tipple et al., 2013). Plant-water D/H composition and plant-wax δD values are largely controlled by the isotopic composition of precipitation (δD_w) (Sachse et al., 2004, 2006; Hou et al., 2008; Feakins and Sessions, 2010; Garcin et al., 2012). δD_{wax} is strongly influenced by both soil evaporation and transpiration (Smith and Freeman, 2006; Polissar and Freeman, 2010; McInerney et al., 2011) and empirical studies of δD_{wax} in our study area point to an important role for aridity, defined as the ratio of mean annual precipitation (MAP) to potential evapotranspiration (PET) (Douglas et al., 2012). In the Yucatan Peninsula, the isotopic composition of precipitation is largely controlled by the amount effect, with

relatively D-depleted precipitation falling during periods of greater rainfall (Medina-Elizalde et al., 2010). The combined effects of changes in aridity and δD_w on δD_{wax} are complementary in this region, and thus render δD_{wax} a sensitive indicator of hydroclimate change.

Fitting the δD_{wax} record to the PW age model (Figure 5) indicates relatively dry conditions between 1200 to 850 years BP, consistent with other regional paleoclimate records that suggest a series of droughts occurred during this period (Figure 5c,d,e,f). Our Lake Chichancanab δD_{wax} record exhibits high-amplitude variability on the order of 45‰ — equivalent to the isotopic range observed in lake surface sediments across southeastern Mexico and northern Central America (47‰), which spans a large range in annual precipitation (800 to 3300 mm) (Douglas et al., 2012). The preservation of large-amplitude δD_{wax} variability implies that the record is not appreciably damped by mixing of plant waxes with a wide range of ages, and that the age integration of soil plant waxes transported to the basin is relatively minor.

In addition, the δD_{wax} record demonstrates relatively high-amplitude, decadal-scale variability, on the order of 20‰. If this variability reflects decadally cycled plant waxes superimposed on an older millennial-scale record, the original decadal signal would have been substantially attenuated, given the values of f_M consistent with our δD_{wax} record (Figure 7). For example, if f_M is ~0.8 (Figure 8, Scenario 2), decadal signals would be attenuated to 23% of an original record (*see section 3.)*, meaning the observed ~20‰ decadal-scale variability resulted from an original climate signal with ~86‰ in

decadal δD_{wax} variability, which would be unrealistically high-amplitude variability for this region.

An alternative explanation is that high-frequency δD_{wax} variability is imparted by millennially cycled plant waxes. This would mean that despite millennial-scale soil residence times, the plant waxes deposited in lake sediments retain unique δD values on decadal time scales, which would require high values for f_M and very low values for σ_M (Figure 8, Scenario 3). In this scenario, the observed decadal variability would be less attenuated (~63% of the original signal; *see section 3.4.2*), implying an original signal with a more plausible 30‰ range in decadal δD_{wax} variability. When fit to the PW age model, the δD_{wax} record shows the highest-amplitude, short-term variability between 1200 and 850 years BP (Figure 5b), consistent with Lake Chichancanab density (Figure 5c) and Chaac speleothem $\delta^{18}O$ (Figure 5e) records.

In summary, both multi-proxy comparisons and modeling indicate that Lake Chichancanab plant-wax age distributions are characterized by high values of f_M and low values of σ_M. This type of age distribution implies that fitting the Lake Chichancanab δD_{wax} record to the PW age-depth model provides a relatively accurate representation of millennial-scale climate change, although this record could be damped and broadened to some extent (Figure 8). The interpretation of decadal δD_{wax} variability is less certain, although we suggest that it is also likely to be primarily imparted by millennially cycled plant waxes, and that the PW age model also provides a reasonably accurate representation of higher-frequency δD_{wax} variability.

4.6 Implications for paleoclimate studies

Few studies have sought to reconstruct plant-wax stable isotope records on centennial or finer timescales. In one example, δD records from both long-chain *n*-alkanoic acids and *n*-alkanes in Santa Barbara Basin sediments from the past 1400 years did not correspond to tree-ring records of regional climate (Li et al., 2011). That study attributed the absence of a coherent δD_{wax} climate record to long soil-residence times of plant waxes in catchment soils, creating a highly mixed δD signal. This assertion is corroborated by $\Delta^{14}C_{wax}$ data indicating the deposition of substantially pre-aged plant waxes in the Santa Barbara Basin (Mollenhauer and Eglinton, 2007). Russell et al. (2009) reported that a late Holocene δD_{wax} record from Lake Wandakara, Uganda was not consistently coherent with other regional paleoclimate records, and argued that discrepancies reflected effects of anthropogenic vegetation shifts, as recorded by $\delta^{13}C_{wax}$, which led to shifts in the apparent D/H fractionation for plant waxes that were independent of climate. An alternative hypothesis to explain the discrepancies between the proxy climate records is that soil storage of plant waxes produced time lags between the Lake Wandakara δD_{wax} and regional paleoclimate records. Notably, recent records of plant-wax δD values over the past 3000 years from two lakes in the Dominican Republic provide a climate signal that is coherent with other regional climate records (Lane et al., 2014).

Although plant-wax isotope records are valuable tools for detecting terrestrial climate change, long-term soil storage has the potential to complicate interpretations at a high temporal resolution. Datasets of $\Delta^{14}C_{wax}$ measurements at the sites of paleoclimate

studies are imperative for testing and resolving such complications. Variability in MRT_{wax} at Lake Chichancanab (Figure 4b) suggests that the application of a constant age offset to plant-wax isotope records is probably not appropriate for many lakes. Plant-wax age models using multiple, downcore $\Delta^{14}C_{wax}$ measurements, as applied in this study, will in some cases provide the best means to develop temporally accurate plant-wax stable isotope records. However, time-integration of plant-wax isotope records in some settings could make interpretations difficult, even with a plant-wax age model, particularly if f_M is relatively low or σ_M is high (e.g. Figure 8 Scenario 1).

It is also possible that many lakes do not contain large amounts of pre-aged plant waxes. For example, large lakes with depocenters far from the lake margin could have a higher proportion of plant waxes rapidly transported as aerosols, in which case pre-aged plant waxes would be much less abundant in sediment cores. Likewise, sediment cores from lakes with small catchments, where a large proportion of terrigenous organic carbon is derived from fresh vegetation deposited directly into the lake, could also be good candidates for study, as suggested by the relatively close agreement between plant-wax and macrofossil radiocarbon ages at Ordy Pond, Hawaii (Uchikawa et al., 2008). Lakes dominantly fed by surface runoff, as opposed to groundwater, could be less likely to contain significant concentrations of pre-aged plant waxes. Plant-wax stable isotope records from marginal marine settings, where data indicate very large MRT_{wax} values, could be especially difficult to interpret on short time-scales. Ultimately, a global dataset of compound-specific radiocarbon ages from both lake and marginal marine sediments would be valuable for identifying the environmental settings that most likely contain low proportions of pre-aged plant waxes.

5. Conclusions

Plant waxes with negative $\Delta^{14}C$ values are found in surficial lake sediments across southeastern Mexico and northern Guatemala, suggesting that pre-aged plant waxes could be widespread in many lake sediments. $^{14}C_{wax}$ data from Lake Chichancanab catchment soils indicate that plant-wax ages increase with soil depth, and that pre-aged plant waxes in the lake sediments are likely derived from deep (≥ 1 meter) soil horizons, suggesting that plant waxes could be transported through subsurface soils. The δD_{wax} record from Lake Chichancanab is coherent with other regional paleoclimate records when fit with the PW age model, as opposed to the TM age model. Furthermore, inverse modeling results suggest that the Lake Chichancanab $\Delta^{14}C_{wax}$ and δD_{wax} data are consistent with most plant-waxes (>75%) being derived from a millennial-aged pool characterized by a relatively narrow range of ages (σ_M < 200 years). These results indicate that the input of pre-aged plant waxes strongly affects the chronology of plant-wax stable isotope records at this lake, and that applying the PW age model provides a reasonable record of past climate change on millennial to centennial timescales.

Acknowledgments We wish to thank Daniel Montluçon, Li Xu and Ann McNichol for assistance with compound-specific radiocarbon measurements, and Gerard Olack, Glendon Hunsinger and Dominic Colosi for assistance with compound-specific stable isotope measurements. Hagit Affek provided helpful comments on an earlier version of the manuscript, and Rienk Smittenberg and an anonymous reviewer provided

constructive reviews. Funding for this research was provided by the U.S. National Science Foundation Graduate Research Fellowship.

References

Aravena R., Warner B. G., MacDonald G. M., Hanf K. I. (1992) Carbon isotope composition of lake sediments in relation to lake productivity and radiocarbon dating. Quaternary Research **37**, 333-345.

Barr D. R., Sherrill E. T. (1999) Mean and variance of truncated normal distributions. The American Statistician **53**, 357-361.

Bauer-Gottwein P., Gondwe B. R., Charvet G., Marín L. E., Rebolledo-Vieyra M., Merediz-Alonso G. (2011) Review: The Yucatán Peninsula karst aquifer, Mexico. Hydrogeology Journal **19**, 507-524.

Bengtsson G., Enfield C. G., Lindqvist R. (1987) Macromolecules facilitate the transport of trace organics. Science of the Total Environment **67**, 159-164.

Berke M. A., Johnson T. C., Werne J. P., Grice K., Schouten S., Sinninghe Damsté J. S. (2012) Molecular records of climate variability and vegetation response since the late Pleistocene in the Lake Victoria Basin, East Africa. Quaternary Science Reviews **55**, 59-74.

Blaauw M. (2010) Methods and code for 'classical' age-modelling of radiocarbon sequences. Quaternary Geochronology **5**, 512-518.

Breckenridge A. J., 2000. Using paleolimnological methods to document Maya landscape alteration: Case studies from the Rio de la Pasion Valley, Peten, Guatemala, Department of Earth Sciences. University of Minnesota, p. 172.

Bull I. D., Bergen P. F. v., Nott C. J., Poulton P. R., Evershed R. P. (2000) Organic geochemical studies of soils from the Rothamsted classical experiments—v. The fate of lipids in different long-term experiments. Organic Geochemistry **31**, 389-408.

Chikaraishi Y., Naraoka H., Poulson S. R. (2004) Hydrogen and carbon isotopic fractionations of lipid biosynthesis among terrestrial (C_3, C_4 and CAM) and aquatic plants. Phytochemistry **65**, 1369-1381.

Colina-Tejada A., Amblès A., Jambu P. (1996) Nature and origin of soluble lipids shed into the soil by rainwater leaching a forest cover of *pinus maritima sp.* European Journal of Soil Science **47**, 637-643.

Crusius J., Anderson R. F. (1995) Sediment focusing in six small lakes inferred from radionuclide profiles. Journal of Paleolimnology **13**, 143-155.

Curtis J. H., Hodell D. A., Brenner M. (1996) Climate variability on the Yucatan Peninsula (mexico) during the past 3500 years, and implications for Maya cultural evolution. Quaternary Research **46**, 37-47.

Deevey, E.S., Brenner, M., Flannery, M.S., Yezdani, G.H. (1980) Lakes Yaxha and Sacnab, Peten, Guatemala: Limnology and hydrology. Archiv für Hydrobiologie **57**,419-460.

Ding G., Rice J. A. (2011) Effect of lipids on sorption/desorption hysteresis in natural organic matter. Chemosphere **84**, 519-526.

Douglas P. M. J., Pagani M., Brenner M., Hodell D. A., Curtis J. H. (2012) Aridity and vegetation composition are important determinants of leaf-wax δD values in southeastern Mexico and Central America. Geochimica Et Cosmochimica Acta **97**, 24-45.

Drenzek N. J., 2007. The temporal dynamics of terrestrial organic matter transfer to the oceans: Initial assessment and application, Joint Program in Oceanograpy/ Applied Ocean Sciences and Engineering. MIT/WHOI Joint Program in Oceanography/ Applied Ocean Sciences and Engineering.

Drenzek N. J., Hughen K. A., Montlucon D. B., Southon J. R., dos Santos G. M., Druffel E. R. M., Giosan L., Eglinton T. I. (2009) A new look at old carbon in active margin sediments. Geology **37**, 239-242.

Drenzek N. J., Montlucon D. B., Yunker M. B., Macdonald R. W., Eglinton T. I. (2007) Constraints on the origin of sedimentary organic carbon in the beaufort sea from coupled molecular ^{13}C and ^{14}C measurements. Marine Chemistry **103**, 146-162.

Eglinton T. I., Aluwihare L. I., Bauer J. E., Druffel E. R. M., McNichol A. P. (1996) Gas chromatographic isolation of individual compounds from complex matrices for radiocarbon dating. Analytical Chemistry **68**, 904-912.

Feakins S. J., Sessions A. L. (2010) Controls on the D/H ratios of plant leaf waxes in an arid ecosystem. Geochimica Et Cosmochimica Acta **74**, 2128-2141.

Feng X., Benitez-Nelson B. C., Montluçon D. B., Prahl F. G., McNichol A. P., Xu L., Repeta D. J., Eglinton T. I. (2012) ^{14}C and ^{13}C characteristics of higher plant biomarkers in washington margin surface sediments. Geochimica Et Cosmochimica Acta **105**, 15-30.

Feng, X., Vonk J. E., van Dongen, B.E., Gustaffson, O., Semilitov, I.P., Dudarev, O. V., Wang, Z., Montluçon, D.B., Wacker, L., and Eglinton, T.I., (2013), Differential mobilization of terrestrial carbon pools in Eurasian Arctic river basins. Proceedings of the National Academy of Sciences **110**, 14168-14173.

Ficken K., Li B., Swain D., Eglinton G. (2000) An *n*-alkane proxy for the sedimentary input of submerged/floating freshwater aquatic macrophytes. Organic Geochemistry **31**, 745-749.

Galy V., Eglinton T. (2011) Protracted storage of biospheric carbon in the Ganges-Brahmaputra basin. Nature Geoscience **4**, 843-847.

Galy V., Eglinton T., France-Lanord C., Sylya S. (2011) The provenance of vegetation and environmental signatures encoded in vascular plant biomarkers carried by the Ganges-Brahmaputra rivers. Earth and Planetary Science Letters **304**, 1-12.

Garcin Y., Schwab V. F., Gleixner G., Kahmen A., Todou G., Séné O., Onana J.-M., Achoundong G., Sachse D. (2012) Hydrogen isotope ratios of lacustrine sedimentary *n*-alkanes as proxies of tropical African hydrology: Insights from a calibration transect across Cameroon. Geochimica Et Cosmochimica Acta **79**, 106-126.

Hassett J. P., Anderson M. A. (1979) Association of hydrophobic organic compounds with dissolved organic matter in aquatic systems. Environmental Science & Technology **13**, 1526-1529.

Hodell D. A., Brenner M., Curtis J. H. (2005) Terminal classic drought in the northern Maya Lowlands inferred from multiple sediment cores in Lake Chichancanab (Mexico). Quaternary Science Reviews **24**, 1413-1427.

Hodell D. A., Brenner M., Curtis J. H. (2007) Climate and cultural history of the northeastern Yucatan Peninsula, Quintana Roo, Mexico. Climatic Change **83**, 215-240.

Hodell D. A., Brenner M., Curtis J. H., Guilderson T. (2001) Solar forcing of drought frequency in the Maya Lowlands. Science **292**, 1367-1370.

Hodell D. A., Curtis J. H., Brenner M. (1995) Possible role of climate in the collapse of Classic Maya Civilization. Nature **375**, 391-394.

Hou J. Z., D'Andrea W. J., Huang Y. S. (2008) Can sedimentary leaf waxes record D/H ratios of continental precipitation? Field, model, and experimental assessments. Geochimica Et Cosmochimica Acta **72**, 3503-3517.

Hughen K. A., Eglinton T. I., Xu L., Makou M. (2004) Abrupt tropical vegetation response to rapid climate changes. Science **304**, 1955-1959.

Kahmen A., Schefuß E., Sachse D. (2013) Leaf water deuterium enrichment shapes leaf wax *n*-alkane δD values of angiosperm plants I: Experimental evidence and mechanistic insights. Geochimica Et Cosmochimica Acta **111**, 39-49.

Kennett D. J., Breitenbach S. F. M., Aquino V. V., Asmerom Y., Awe J., Baldini J. U. L., Bartlein P., Culleton B. J., Ebert C., Jazwa C. (2012) Development and disintegration of Maya political systems in response to climate change. Science **338**, 788-791.

Kohl S. D., Rice J. A. (1999) Contribution of lipids to the nonlinear sorption of polycyclic aromatic hydrocarbons to soil organic matter. Organic Geochemistry **30**, 929-936.

Konecky B. L., Russell J. M., Johnson T. C., Brown E. T., Berke M. A., Werne J. P., Huang Y. (2011) Atmospheric circulation patterns during late Pleistocene climate changes at Lake Malawi, Africa. Earth and Planetary Science Letters **312**, 318-326.

Kusch S., Rethemeyer J., Schefuss E., Mollenhauer G. (2010) Controls on the age of vascular plant biomarkers in Black Sea sediments. Geochimica Et Cosmochimica Acta **74**, 7031-7047.

Lane C. S., Horn S. P., Kerr M. T. (2014) Beyond the Mayan Lowlands: Impacts of the Terminal Classic Drought in the Caribbean Antilles. Quaternary Science Reviews **86**, 89-98.

Leyden B. W. (2002) Pollen evidence for climatic variability and cultural disturbance in the Maya Lowlands. Ancient Mesoamerica **13**, 85-101.

Li C., Sessions A. L., Valentine D. L., Thiagarajan N. (2011) D/H variation in terrestrial lipids from Santa Barbara Basin over the past 1400 years: A preliminary assessment of paleoclimatic relevance. Organic Geochemistry **42**, 15-24.

Matsumoto K., Kawamura K., Uchida M., Shibata Y. (2007) Radiocarbon content and stable carbon isotopic ratios of individual fatty acids in subsurface soil: Implication for selective microbial degradation and modification of soil organic matter. Geochemical Journal **41**, 483-492.

McInerney F. A., Helliker B. R., Freeman K. H. (2011) Hydrogen isotope ratios of leaf wax *n*-alkanes in grasses are insensitive to transpiration. Geochimica Et Cosmochimica Acta **75**, 541-554.

Medina-Elizalde M., Burns S. J., Lea D. W., Asmerom Y., von Gunten L., Polyak V., Vuille M., Karmalkar A. (2010) High resolution stalagmite climate record from the Yucatan Peninsula spanning the Maya Terminal Classic period. Earth and Planetary Science Letters **298**, 255-262.

Medina-Elizalde M., Rohling E. J. (2012) Collapse of Classic Maya Civilization related to modest reduction in precipitation. Science **335**, 956-959.

Mollenhauer G., Eglinton T. I. (2007) Diagenetic and sedimentological controls on the composition of organic matter preserved in California Borderland Basin sediments. Limnology and Oceanography **52**, 558-576.

Naafs D. F., van Bergen P. F., Boogert S. J., de Leeuw J. W. (2004) Solvent-extractable lipids in an acid andic forest soil; Variations with depth and season. Soil Biology and Biochemistry **36**, 297-308.

New M., Lister D., Hulme M., Makin I. (2002) A high-resolution data set of surface climate over global land areas. Climate Research **21**, 1-25.

Nierop K., Buurman P. (1998) Composition of soil organic matter and its water-soluble fraction under young vegetation on drift sand, central Netherlands. European Journal of Soil Science **49**, 605-615.

Ouyang Y., Shinde D., Mansell R., Harris W. (1996) Colloid-enhanced transport of chemicals in subsurface environments: A review. Critical Reviews in Environmental Science and Technology **26**, 189-204.

Pagani M., Pedentchouk N., Huber M., Sluijs A., Schouten S., Brinkhuis H., Damste J. S. S., Dickens G. R., Scientists E. (2006) Arctic hydrology during global warming at the Palaeocene/Eocene thermal maximum. Nature **442**, 671-675.

Perry E., Velazquez-Oliman G., Marin L. (2002) The hydrogeochemistry of the karst aquifer system of the northern Yucatan Peninsula, Mexico. International Geology Review **44**, 191-221.

Pignatello J. J. (2012) Dynamic interactions of natural organic matter and organic compounds. Journal of Soils and Sediments **12**, 1241-1256.

Polissar P. J., Freeman K. H. (2010) Effects of aridity and vegetation on plant-wax δD in modern lake sediments. Geochimica et Cosmochimica Acta **74**, 5785-5797.

Reimer P. J., Bard E., Bayliss A., Beck J. W., Blackwell P. G., Ramsey C. B., Buck C. E., Cheng H., Edwards R. L., Friedrich M. (2013) Intcal13 and Marine13 radiocarbon age calibration curves 0–50,000 years cal BP. Radiocarbon **55**, 1869-1887.

Rosenmeier M. F., Hodell D. A., Brenner M., Curtis J. H., Guilderson T. P. (2002) A 4000-year lacustrine record of environmental change in the southern Maya Lowlands, Peten, Guatemala. Quaternary Research **57**, 183-190.

Rozanski K., Araguás-Araguás L., Gonfiantini R. (1993) Isotopic patterns in modern global precipitation. Geophysical Monograph Series **78**, 1-36.

Russell J. M., McCoy S., Verschuren D., Bessems I., Huang Y. (2009) Human impacts, climate change, and aquatic ecosystem response during the past 2000 yr at Lake Wandakara, Uganda. Quaternary Research **72**, 315-324.

Sachse D., Radke J., Gleixner G. (2004) Hydrogen isotope ratios of recent lacustrine sedimentary n-alkanes record modern climate variability. Geochimica et Cosmochimica Acta **68**, 4877-4889.

Sachse D., Radke J., Gleixner G. (2006) δD values of individual *n*-alkanes from terrestrial plants along a climatic gradient - implications for the sedimentary biomarker record. Organic Geochemistry **37**, 469-483.

Sambridge M. (1999) Geophysical inversion with a neighbourhood algorithm—I. Searching a parameter space. Geophysical Journal International **138**, 479-494.

Schefuss E., Kuhlmann H., Mollenhauer G., Prange M., Patzold J. (2011) Forcing of wet phases in southeast Africa over the past 17,000 years. Nature **480**, 509-512.

Smith F. A., Freeman K. H. (2006) Influence of physiology and climate on δD of leaf wax *n*-alkanes from C_3 and C_4 grasses. Geochimica Et Cosmochimica Acta **70**, 1172-1187.

Smittenberg R. H., Eglinton T. I., Schouten S., Damste J. S. S. (2006) Ongoing buildup of refractory organic carbon in boreal soils during the Holocene. Science **314**, 1283-1286.

Smittenberg R. H., Hopmans E. C., Schouten S., Hayes J. M., Eglinton T. I., Damste J. S. S. (2004) Compound-specific radiocarbon dating of the varved Holocene sedimentary record of Saanich Inlet, Canada. Paleoceanography **19**.

Tierney J. E., Russell J. M., Huang Y. (2010) A molecular perspective on late quaternary climate and vegetation change in the Lake Tanganyika Basin, East Africa. Quaternary Science Reviews **29**, 787-800.

Tierney J. E., Russell J. M., Huang Y. S., Damste J. S. S., Hopmans E. C., Cohen A. S. (2008) Northern hemisphere controls on tropical southeast African climate during the past 60,000 years. Science **322**, 252-255.

Tierney J. E., Russell J. M., Sinninghe Damsté J. S., Huang Y., Verschuren D. (2011) Late Quaternary behavior of the East African monsoon and the importance of the Congo air boundary. Quaternary Science Reviews **30**, 798-807.

Tipple B. J., Berke M. A., Doman C. E., Khachaturyan S., Ehleringer J. R. (2013) Leaf-wax *n*-alkanes record the plant–water environment at leaf flush. Proceedings of the National Academy of Sciences **110**, 2659-2664.

Tipple B. J., Pagani M. (2010) A 35myr north american leaf-wax compound-specific carbon and hydrogen isotope record: Implications for C_4 grasslands and hydrologic cycle dynamics. Earth and Planetary Science Letters **299**, 250-262.

Torn M. S., Trumbore S. E., Chadwick O. A., Vitousek P. M., Hendricks D. M. (1997) Mineral control of soil organic carbon storage and turnover. Nature **389**, 170-173.

Trumbore S. (2000) Age of soil organic matter and soil respiration: Radiocarbon constraints on belowground C dynamics. Ecological Applications **10**, 399-411.

Trumbore S. E., Davidson E. A., de Camargo P. B., Nepstad D. C., Martinelli L. A. (1995) Belowground cycling of carbon in forests and pastures of Eastern Amazonia. Global Biogeochemical Cycles **9**, 515-528.

Uchida M., Shibata Y., Ohkushi K., Yoneda M., Kawamura K., Morita M. (2005) Age discrepancy between molecular biomarkers and calcareous foraminifera isolated from the same horizons of northwest Pacific sediments. Chemical Geology **218**, 73-89.

Uchikawa J., Popp B. N., Schoonmaker J. E., Xu L. (2008) Direct application of compound-specific radiocarbon analysis of leaf waxes to establish lacustrine sediment chronology. Journal of Paleolimnology **39**, 43-60.

Veldkamp E., Becker A., Schwendenmann L., Clark D. A., Schulte-Bisping H. (2003) Substantial labile carbon stocks and microbial activity in deeply weathered soils below a tropical wet forest. Global Change Biology **9**, 1171-1184.

Vonk J. E., van Dongen B. E., Gustafsson O. (2010) Selective preservation of old organic carbon fluvially released from sub-arctic soils. Geophysical Research Letters **37**.

Waldner G., Friesl-Hanl W., Haberhauer G., Gerzabek M. H. (2012) Differences in sorption behavior of the herbicide 4-chloro-2-methylphenoxyacetic acid on artificial soils as a function of soil pre-aging. Journal of Soils and Sediments **12**, 1292-1298.

Wieland E., Santschi P. H., Beer J. (1991) A multitracer study of radionuclides in Lake Zurich, Switzerland: 2. Residence times, removal processes, and sediment focusing. Journal of Geophysical Research: Oceans **96**, 17067-17080.

Figure Captions

Figure 1. A) Map of the Yucatan Peninsula and northern Central America showing the location of sites discussed in the text; **B)** Map of Lake Chichancanab and its catchment. Elevation data are from the Shuttle Radar Topography Mission. The green line indicates the approximate perimeter of the lake catchment; the lake is colored blue. Orange letters indicate the location of soil sampling sites. The red circle indicates the location of the lake sediment core.

Figure 2. $\Delta^{14}C_{wax}$ in lake surface sediments versus annual precipitation. $\Delta^{14}C_{wax}$ values are negative for all four lakes, indicating plant waxes in surficial sediments do not incorporate a significant amount of 'post-bomb' carbon from later than 1950. $\Delta^{14}C_{wax}$ in lake surface sediments appears to be positively correlated with annual precipitation (A), and negatively correlated with catchment area (B). Error bars indicate analytical, blank-corrected error for $\Delta^{14}C_{wax}$.

Figure 3. $^{14}C_{wax}$ in Lake Chichancanab catchment soils versus soil depth. At sites A and B $\Delta^{14}C_{wax}$ decreases with soil depth. Soils from site B, on the east side of the lake, have lower plant-wax $\Delta^{14}C_{wax}$ values for a given soil depth. None of the soils have $\Delta^{14}C_{wax}$ values as low as the lake surface sediments from Lake Chichancanab, indicated by the orange bar. Light dashed lines indicate the depth at which $\Delta^{14}C_{wax}$ values from Sites A and B would intersect lake surface sediment $\Delta^{14}C_{wax}$, assuming a linear decrease in $\Delta^{14}C_{wax}$ with soil depth in subsoil horizons. Error bars indicate analytical error in $\Delta^{14}C_{wax}$ measurements. The black dashed line indicates the current $\Delta^{14}C$ value of atmospheric CO_2.

Figure 4. A) Lake Chichancanab age-depth models based on calibrated radiocarbon ages for plant waxes (PW; green; left) and terrigenous macrofossils (TM; red; right). The age probability density of individual radiocarbon analyses is shown. The black lines indicate the 'best' age model or mean of all age-model iterations, and the colored bands indicate the 95% confidence intervals. The PW and TM age models do not overlap at any point. **B)** The mean soil residence time of plant waxes (MRT_{wax}) plotted against core depth. MRT_{wax} is the difference between the age of plant waxes derived from the PW age-depth model and the age of sediment deposition derived from the TM age-depth model. These values assume that plant waxes are primarily derived from catchment soils (*See sections 4.3 and 4.4*). The error bars and error envelope indicate propagated uncertainty from the 95% confidence intervals for the PM and TM age models.

Figure 5. Comparison of the Lake Chichancanab δD_{mean} record with regional paleoclimate records. (**A**) δD_{wax} fit to the TM age model; (**B**) δD_{wax} fit to the PW age model; (**C**) Lake Chichancanab sediment density (Hodell et al., 2005); (**D**) Lake Chichancanab snail (*Pyrgophorus*) $\delta^{18}O$ (Hodell et al., 1995); (**E**) Chaac speleothem $\delta^{18}O$ (Medina-Elizalde et al., 2010); (**F**) Punta Laguna ostracod (*Cytheridella ilosvayi*) $\delta^{18}O$ (Curtis et al., 1996). The latter five climate records (**B, C, D, E, F)** all indicate a period of drought between 1200 and 850 BP (marked in yellow). Arrows highlight a long-term drying trend between 2200 and 1200 BP apparent in records **B**, **D** and **E**.

Figure 6. Comparison of Lake Chichancanab sediment core MRT_{wax} data with (**A**) δD_{wax} and (**B**) $\delta^{13}C_{wax}$ values. No relationship is observed between these variables. The mean and standard deviation of δD and $\delta^{13}C$ values from regional aquatic plants, regional soils, and Lake Chichancanab catchment soils are also plotted (without reference to the x-axis). Aquatic plant and Lake Chichancanab catchment soil stable isotope data are given in Supplemental Tables S2 and S3; regional soil stable isotope data are from Douglas et al. (2012). Lake Chichancanab sedimentary plant wax stable isotope data generally overlap with soil samples, and are not consistent with emergent aquatic plants being a major source.

Figure 7. Results of inverse model runs in which (**A**) f_M and σ_M and (**B**) μ_M and σ_M are free parameters. These results are from models with $k = 12$ and the δD_{wax} record smoothed with a three-point moving average, and are representative of models run with other data inputs (Table 4). The color bar indicates the correlation coefficient (r) between δD_{wax} and δ_{ynth} for each set of free parameters, and applies to both plots. White spaces in (**B**) indicate sets of parameters that cannot reproduce the observed variability in MRT_{wax}. In (**A**) the best model fits occur with relatively high values of f_M (> 0.75) and low values of σ_M (< 200). In (**B**) the best model fits occur at the edge of the range of permissible values, with the lowest possible values of μ_M. Overall, the age distributions in (**A**) produce a better fit to the δD_{wax} record than the age distributions in (**B**).

Figure 8. Effects of different plant-wax age distributions on a synthetic climate record. (**A**) The three plant-wax age distributions considered. Parameters held constant are listed in black, and the unique parameters for each age distribution are listed in the corresponding color. (**B**) The outcome of filtering the simplified climate record, shown in black, through these three age distributions; the colors of the curves correspond to the age distributions in (**A**). (**C**) as in (**B**), but the filtered records are shifted back in time by 700 years to account for the MRT_{wax} value, equivalent to the effect of applying a plant-wax (PW) age model.

Table 1. Location, climatic and geomorphologic characteristics of the studied lakes.

Lake	Latitude (°	Longitude (°	Annual	Catchment	Catchment

	N)	W)	Precipitation (mm)	Area (km^2)	Relief (m)
Chichancanab	19.87	88.77	1161	137.07	50
Punta Laguna	20.65	87.64	1330	0.92	22
Salpeten	16.98	89.67	1717	7.34	205
Itzan	16.6	90.48	2098	1.51	80

Table 2. Lake Surface Sediment and Soil $^{14}C_{wax}$ Results.

Sample	NOSAMS Sample Number	$\Delta^{14}C_{wax}$ (‰)	Error	$\delta^{13}C_{NOSAMS}$	$\delta^{13}C_{GC\text{-}IRMS}$
Lake Surface Sediments					
Chichancanab	80694	-69	9	-30.3	-30.7
Punta Laguna	80698	-23	12	-33.2	-33.6
Salpeten	88449	-8	18	-32.9	N/A
Itzan	108085	-10	7	-39.7	-39.1
Lake Chichancanab Catchment Soils					
Site A 5 cm	112590	119	6	-33.6	-32.7
Site A 40 cm	112591	-12	5	-32.7	-32
Site A 70 cm	112592	-39	27	N/A	-32.2
Site B 20 cm	112593	-18	8	-33.3	-32.8
Site B 50 cm	112594	-44	9	-33.1	-32.4
Site C	112589	40	10	-24.48	-25.1

Table 3: Lake Chichancanab Sediment Core $^{14}C_{wax}$ Results

Sample	NOSAMS Sample Number	$\Delta^{14}C_{wax}$ (‰)	Error	Cal Age[a] (Years BP) 2σ range	$\delta^{13}C_{NOSAMS}$	$\delta^{13}C_{GC-IRMS}$	Sediment Core Age[b] (Cal Yr BP) 95% CI	MRT_{wax} (Years) 95% CI
Coretop	80694	-69	9	(334) 548 (665)	-30.3	-30.7	(-76) -58 (-49)	(490) 617 (715)
50-54 cm	80708	-116	8	(727) 849 (964)	-31.2	-30.9	(213) 258 (299)	(423) 554 (682)
100-104 cm	80704	-120	14	(678) 879 (1172)	-31.4	-31.4	(597) 650 (701)	(268) 412 (616)
119-123 cm	75491	-166	14	(1059) 1316 (1553)	-31.7	-31.3	(772) 822 (870)	(222) 352 (508)
144-148 cm	80701	-173	8	(1289) 1371 (1522)	-30.8	-30.5	(1026) 1067 (1104)	(303) 390 (531)
161-165 cm	*75494*	*-428*	*11*	*(4860) 5063 (5296)*	*-30.2*	*-31.6*		
170-172 cm r1	107492	-224	6	(1824) 1943 (2099)	-30.9	-29.9	(1294) 1334 (1367)	(483) 565 (663)
170-172 cm r2	109664	-223	11	(1708) 1926 (2148)	-30.2	-29.9		
194-197 cm	75497	-253	12	(2044) 2307 (2701)	-29.6	-29.4	(1573) 1622 (1676)	(627) 747 (915)
211-215 cm	*75499*	*-409*	*8*	*(4530) 4705 (4847)*	*-33*	*-30.2*		
243-245 cm	75502	-334	10	(3236) 3437	-31.1	-30.3	(2124) 2238	(960) 1185

				(3612)			(2382)	(1465)

Italics indicate samples whose $\delta^{13}C$ values indicate likely contamination
[a]Center value indicates median probability age.
[b]Center value indicates 'best' age estimate, or mean of age model iterations.
[c]Center value indicates difference between plant-wax calibrated age and sediment core age.

Table 4: Best-fit solutions for inverse models with different data inputs and free parameters.

Free Parameters	k	δD_{wax} Smoothing	f_M	σ_M (Years)	r	R^2
f_M, σ_M	8	3 point average	0.83	79	0.71	0.51
f_M, σ_M	12	3 point average	0.83	79	0.71	0.51
f_M, σ_M	16	3 point average	0.83	79	0.71	0.51
f_M, σ_M	12	none	0.83	79	0.71	0.51
f_M, σ_M	12	5 point average	0.83	80	0.71	0.51
f_M, σ_M	12	100-year bins	0.83	79	0.71	0.51
Free Parameters	k	δD_{wax} Smoothing	μ_M (Years)	σ_M (Years)	r	R^2
μ_M, σ_M	8	3 point average	1342	5	0.63	0.40
μ_M, σ_M	12	3 point average	1342	8	0.63	0.40
μ_M, σ_M	16	3 point average	1342	7	0.63	0.40
μ_M, σ_M	12	none	1342	5	0.64	0.40
μ_M, σ_M	12	5 point average	1345	11	0.61	0.38
μ_M, σ_M	12	100-year bins	1344	18	0.60	0.37

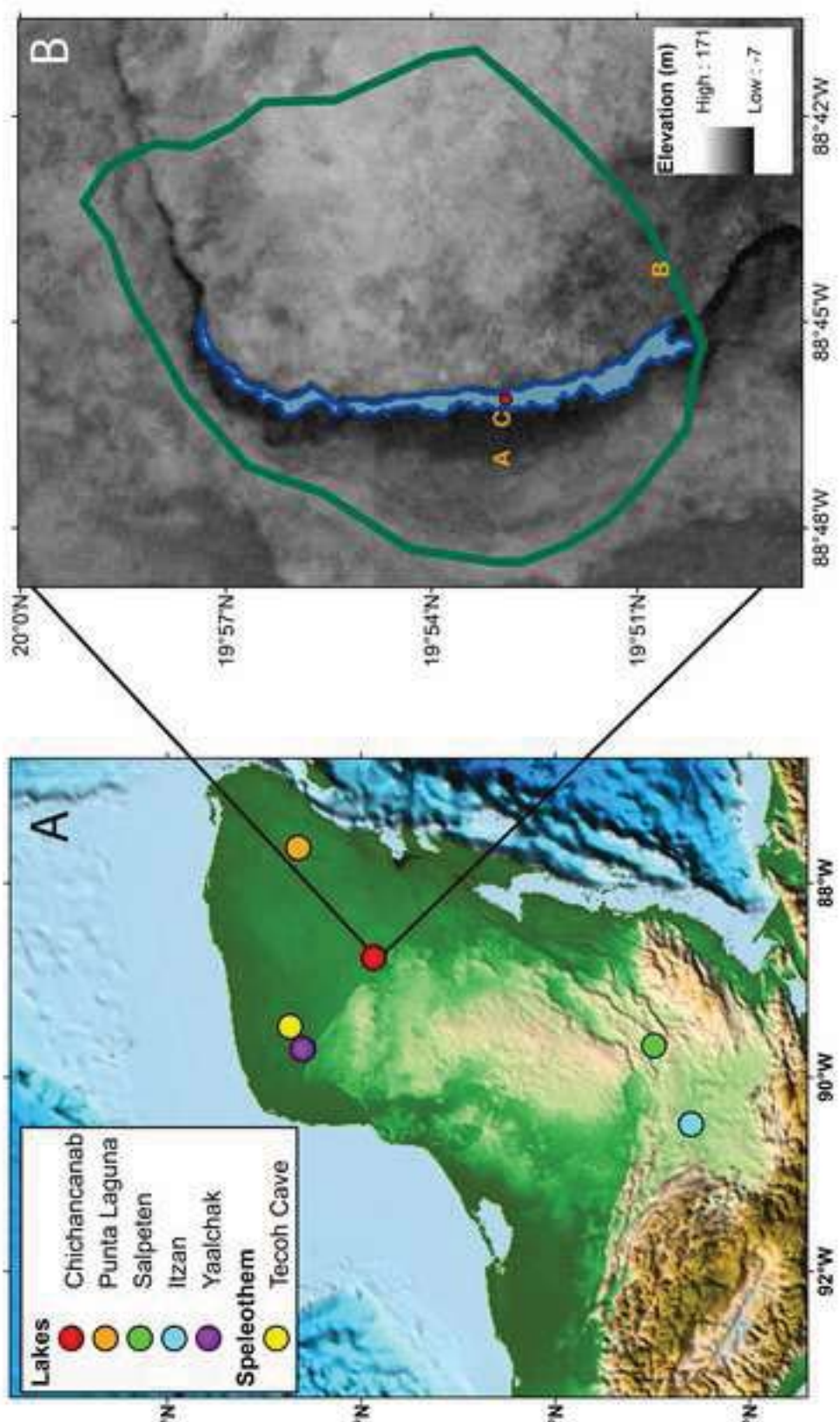

Figure(s)

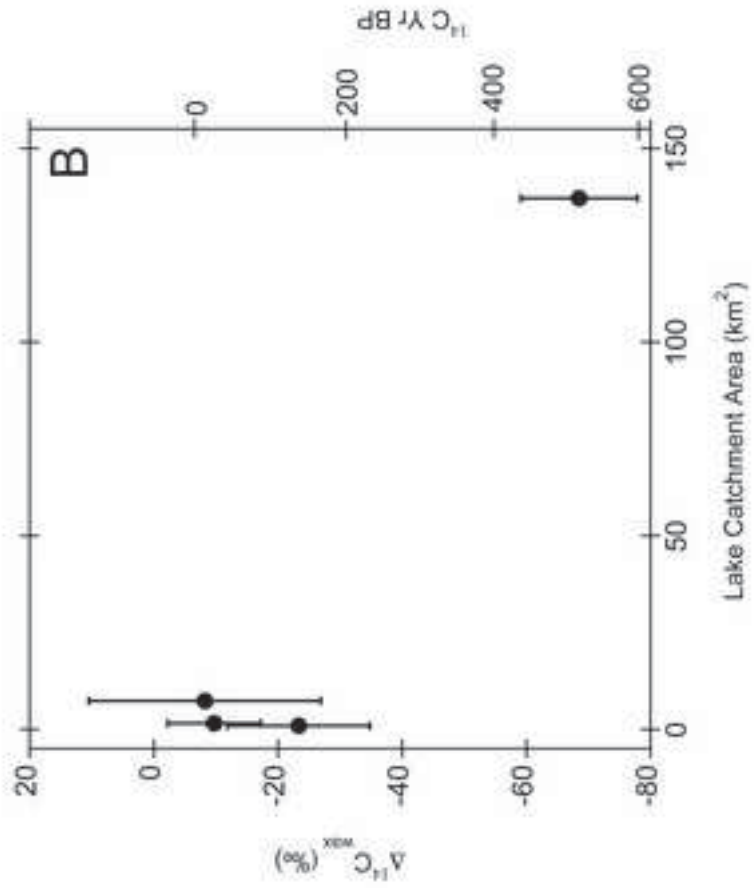

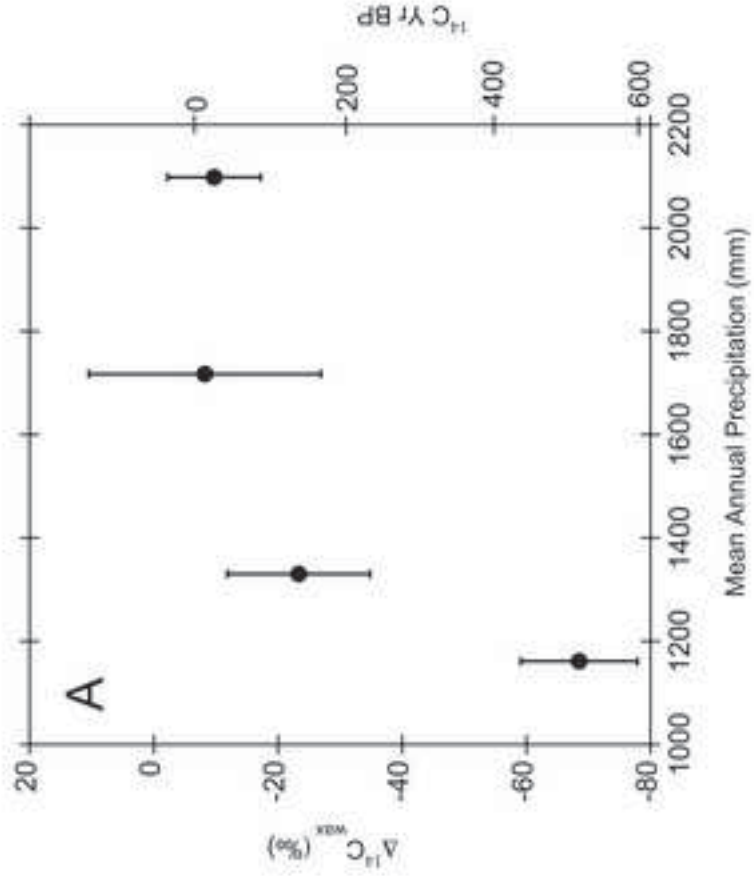

Figure

Figure

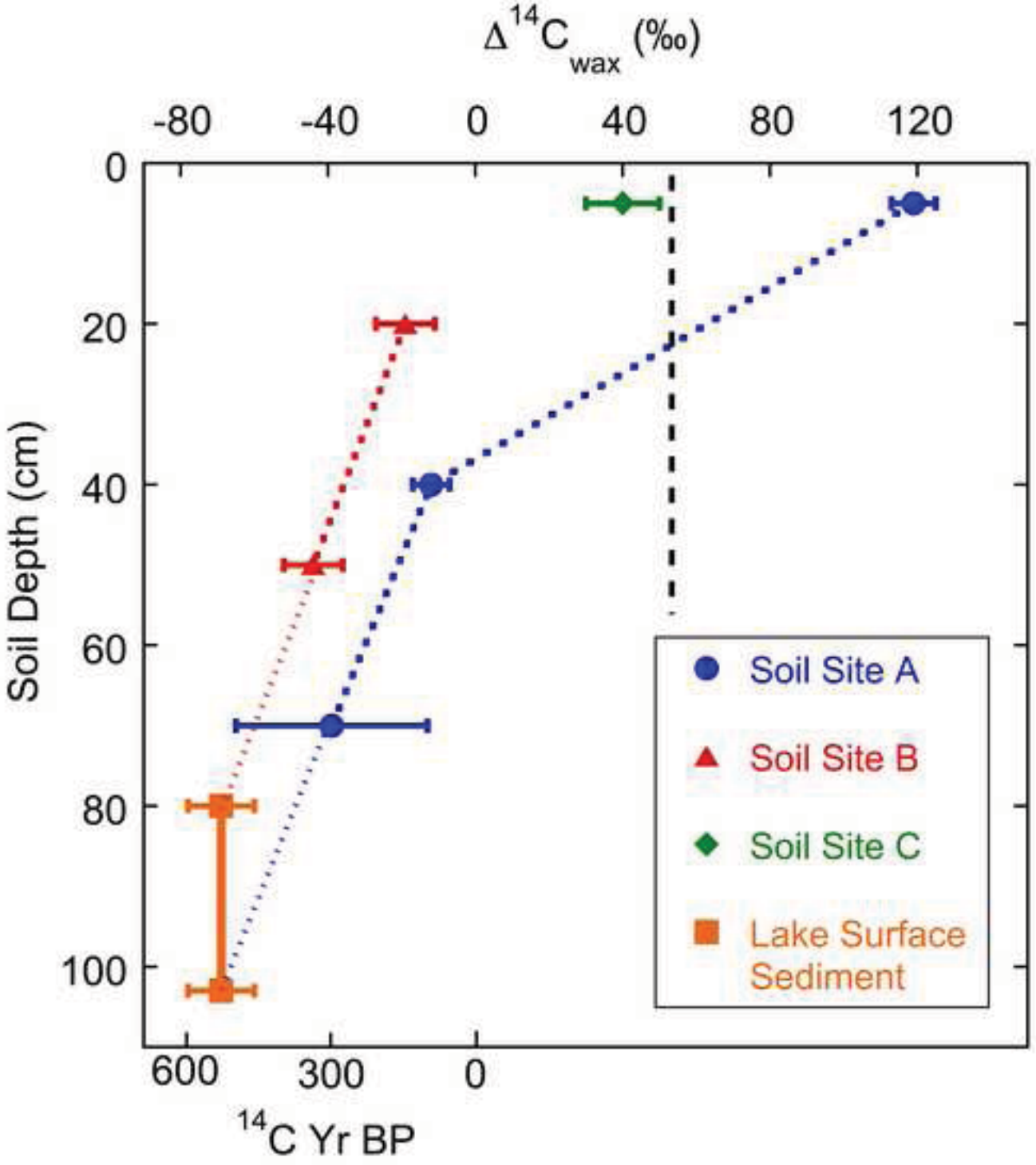

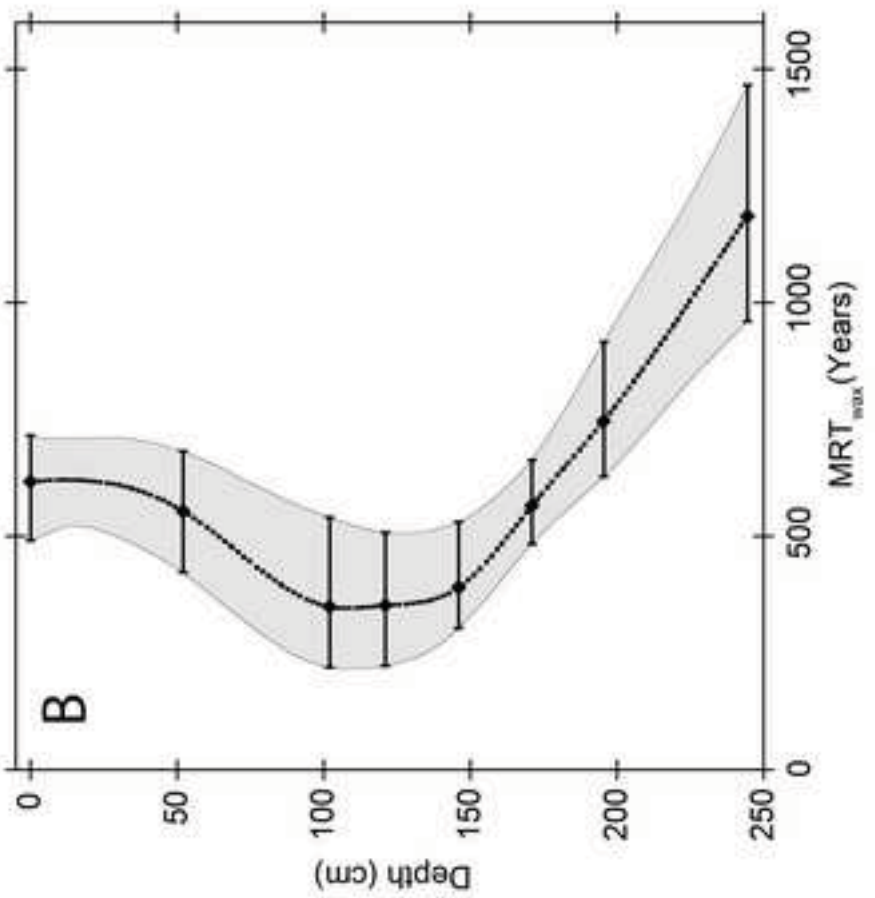

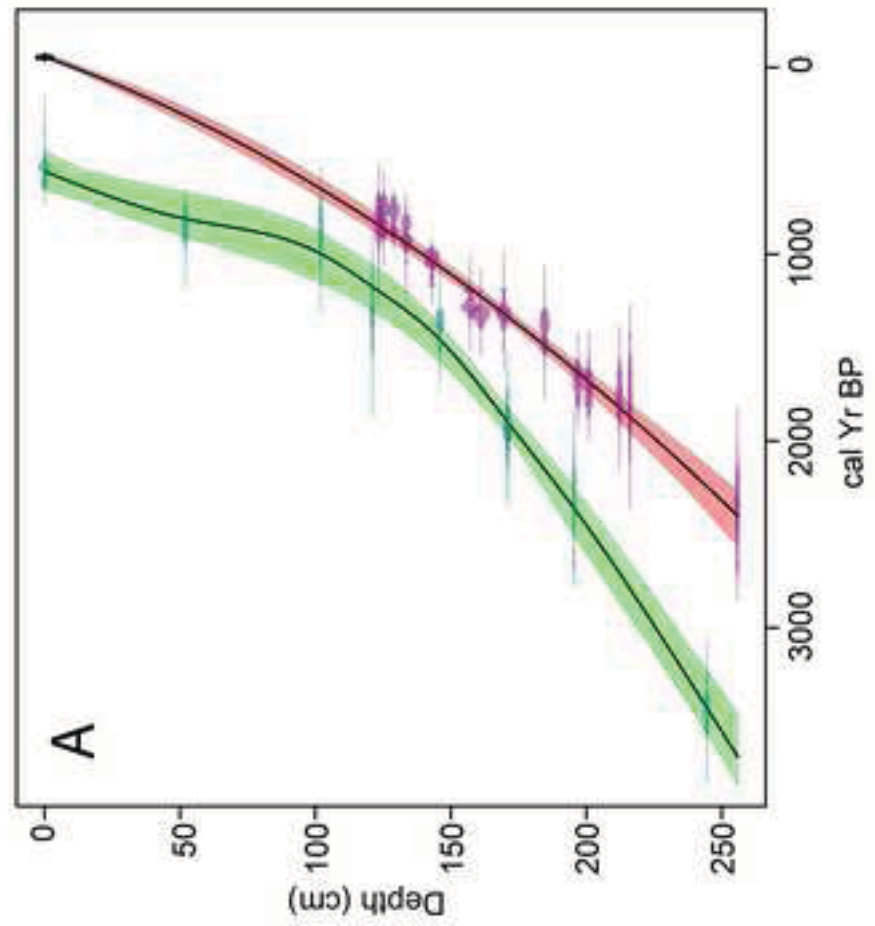

Figure(s)

Figure(s)

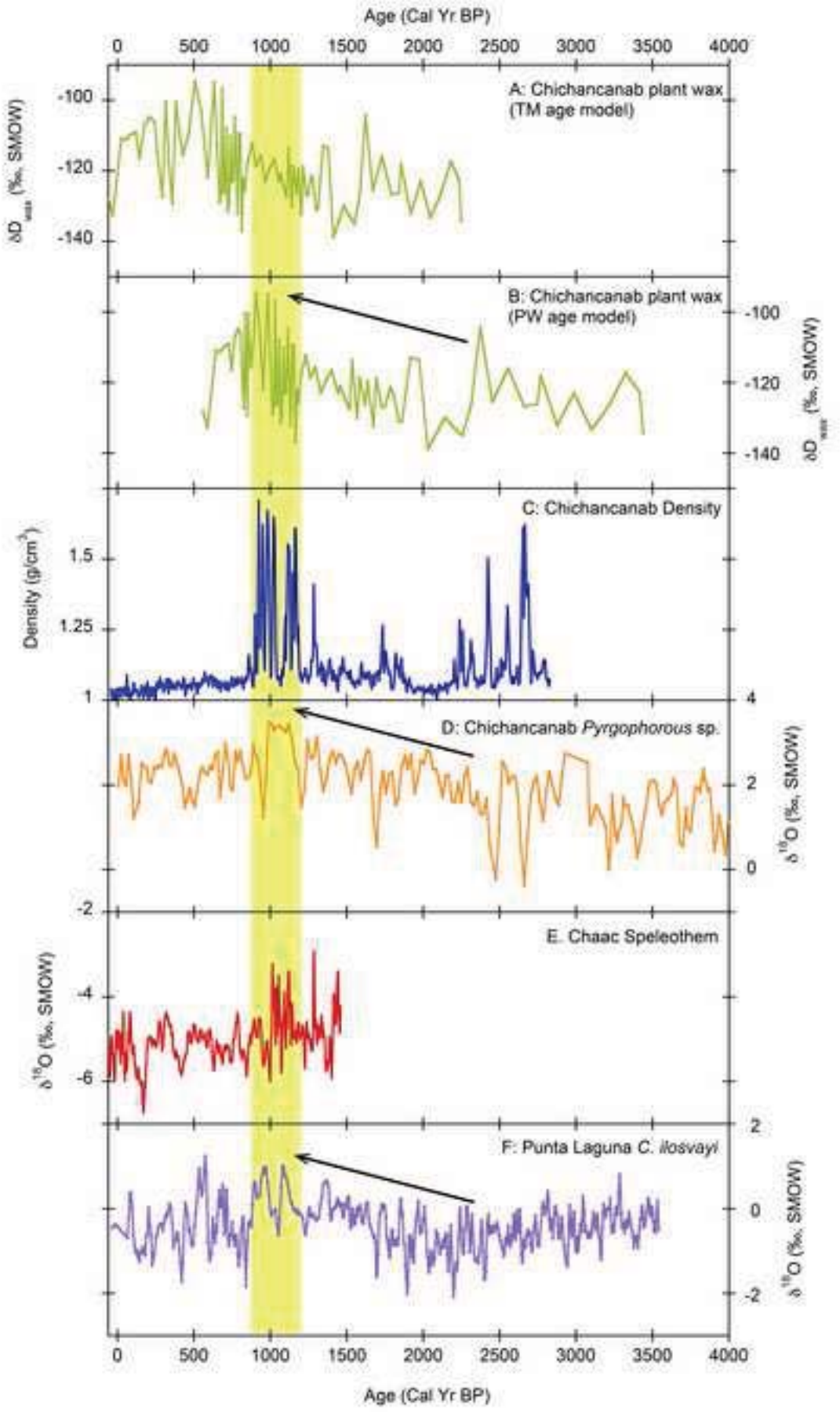

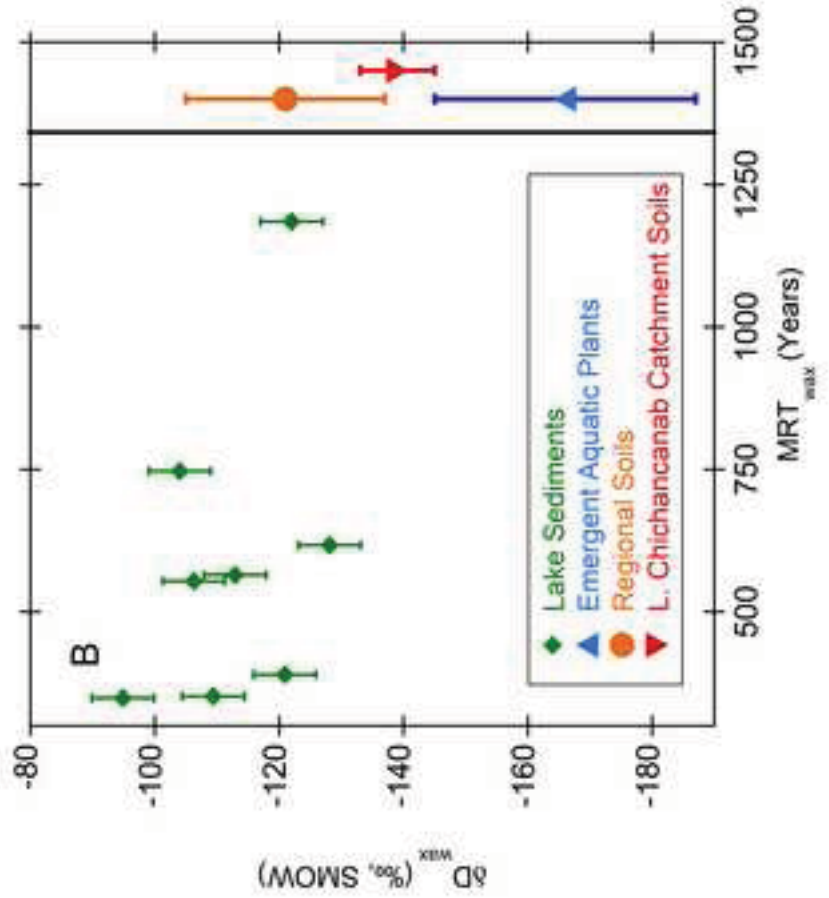

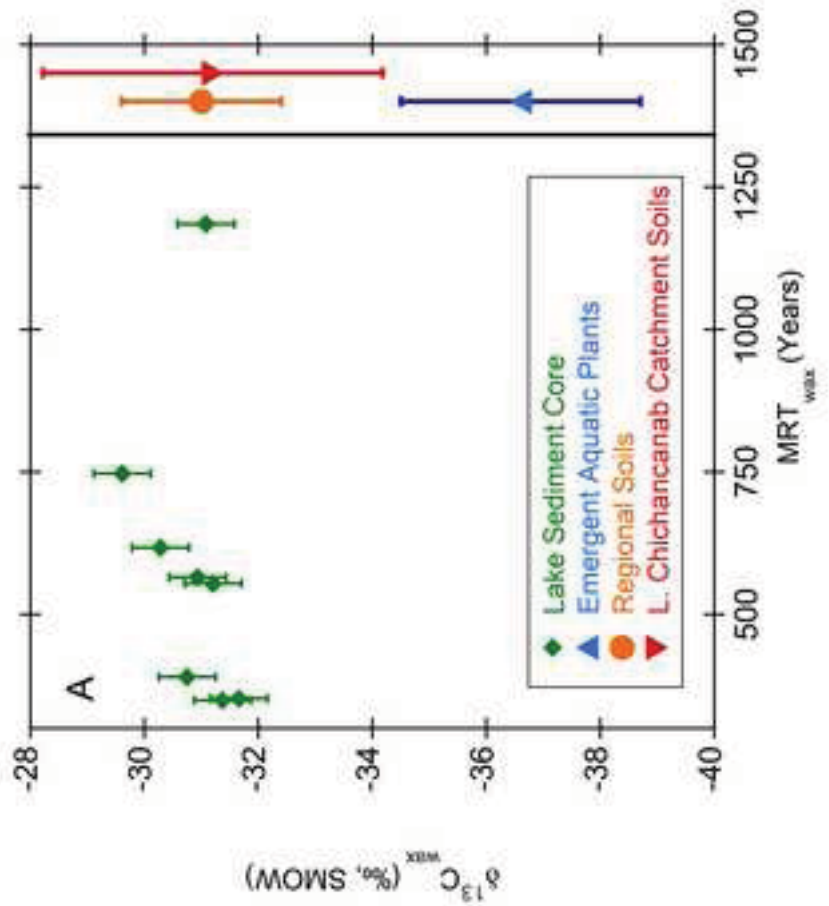

Figure(s)

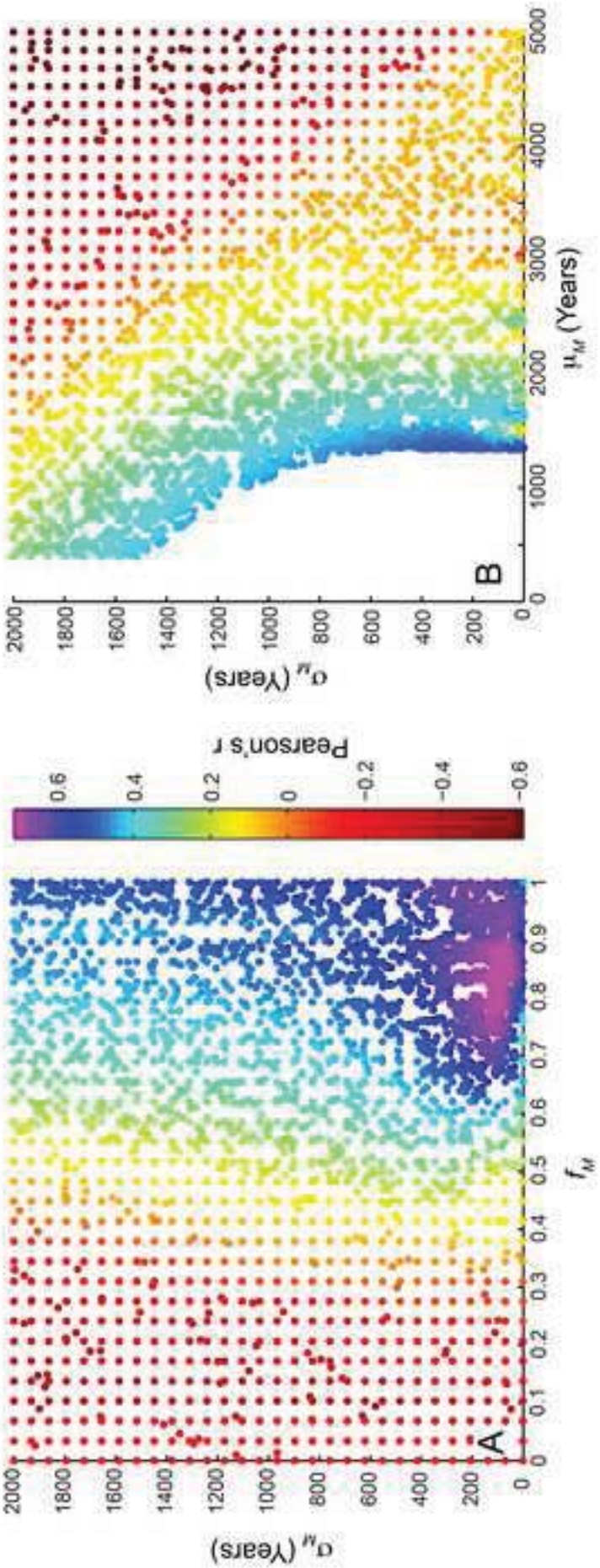

Figure(s)